Brain, Behavior, & Immunity - Health 40 (2024) 100823

Contents lists available at ScienceDirect

Brain, Behavior, & Immunity - Health

journal homepage: www.editorialmanager.com/bbih/default.aspx

Lung-brain crosstalk: Behavioral disorders and neuroinflammation in septic survivor mice

Kelly Cattelan Bonorino [a], Scheila Iria Kraus [a], Gisele Henrique Cardoso Martins [a], Jéssica Jorge Probst [b], Débora Melissa Petry Moeke [c], Alice Henrique dos Santos Sumar [d], Yuri Reis Casal [e], Filipe Rodolfo Moreira Borges Oliveira [f], Regina Sordi [f], Jamil Assreuy [f], Morgana Duarte da Silva [a], Deborah de Camargo Hizume Kunzler [g,*]

[a] Neurosciences, Federal University of Santa Catarina Brazil, Brazil
[b] Federal University of Santa Catarina, Postgraduate Program in Biochemistry, Brazil
[c] Department of Physical Therapy, University of British Columbia, Canada
[d] Medical Sciences, Federal University of Santa Catarina, Brazil
[e] Neuropathology, Department of Pathology, Medical School Hospital of the São Paulo University, Brazil
[f] Department of Pharmacology, Center of Biological Sciences, Federal University of Santa Catarina, Brazil
[g] Department of Physical Therapy, Santa Catarina State University, Brazil

ARTICLE INFO

Keywords:
Sepsis
Lung inflammation
Neuroinflammation
Behavior

ABSTRACT

Although studies have suggested an association between lung infections and increased risk of neuronal disorders (e.g., dementia, cognitive impairment, and depressive and anxious behaviors), its mechanisms remain unclear. Thus, an experimental mice model of pulmonary sepsis was developed to investigate the relationship between lung and brain inflammation. Male Swiss mice were randomly assigned to either pneumosepsis or control groups. Pneumosepsis was induced by intratracheal instillation of *Klebsiella pneumoniae*, while the control group received a buffer solution. The model's validation included assessing systemic markers, as well as tissue vascular permeability. Depression- and anxiety-like behaviors and cognitive function were assessed for 30 days in sepsis survivor mice, inflammatory profiles, including cytokine levels (lungs, hippocampus, and prefrontal cortex) and microglial activation (hippocampus), were examined. Pulmonary sepsis damaged distal organs, caused peripheral inflammation, and increased vascular permeability in the lung and brain, impairing the blood-brain barrier and resulting in bacterial dissemination. After sepsis induction, we observed an increase in myeloperoxidase activity in the lungs (up to seven days) and prefrontal cortex (up to 24 h), proinflammatory cytokines in the hippocampus and prefrontal cortex, and percentage of areas with cells positive for ionized calcium-binding adaptor molecule 1 (IBA-1) in the hippocampus. Also, depression- and anxiety-like behaviors and changes in short-term memory were observed even 30 days after sepsis induction, suggesting a crosstalk between inflammatory responses of lungs and brain.

1. Introduction

Sepsis is a life-threatening organ dysfunction caused by a dysregulated response to infection (Mervyn et al., 2016; Seymour et al., 2016; M. Singer et al., 2016; Gül et al., 2017; Evans et al., 2021). Also, it is a heterogeneous condition, and patients present organ dysfunctions with variable mortality in short-term hospitalization (Adhikari et al., 2010).

About 48.9 million cases of sepsis per year are estimated worldwide, accounting for 11 million annual deaths (about 19.7% of all deaths) (Rudd et al., 2020). Although short-term mortality and incidence have decreased, sepsis still contributes to considerable morbidity and mortality after hospital discharge (Wilhelms et al., 2010; Fleischmann et al., 2016).

Sepsis survivors may present worsening of previous chronic conditions and increased risk of functional and cognitive impairment and neuropsychiatric disorders (Iwashyna et al., 2010; Prescott and Angus,

* Corresponding author. Centro de Ciências da Saúde e do Esporte - CEFID, Programa de Pós-Graduação em Fisioterapia - PPGFt, Experimental Research Laboratory, LaPEx, 358 Pascoal Simone Street, Coqueiros, Florianópolis, Santa Catarina, 88080-350, Brazil.
E-mail address: dehizume@gmail.com (D. de Camargo Hizume Kunzler).

https://doi.org/10.1016/j.bbih.2024.100823
Received 22 December 2023; Received in revised form 6 June 2024; Accepted 15 July 2024
Available online 2 August 2024

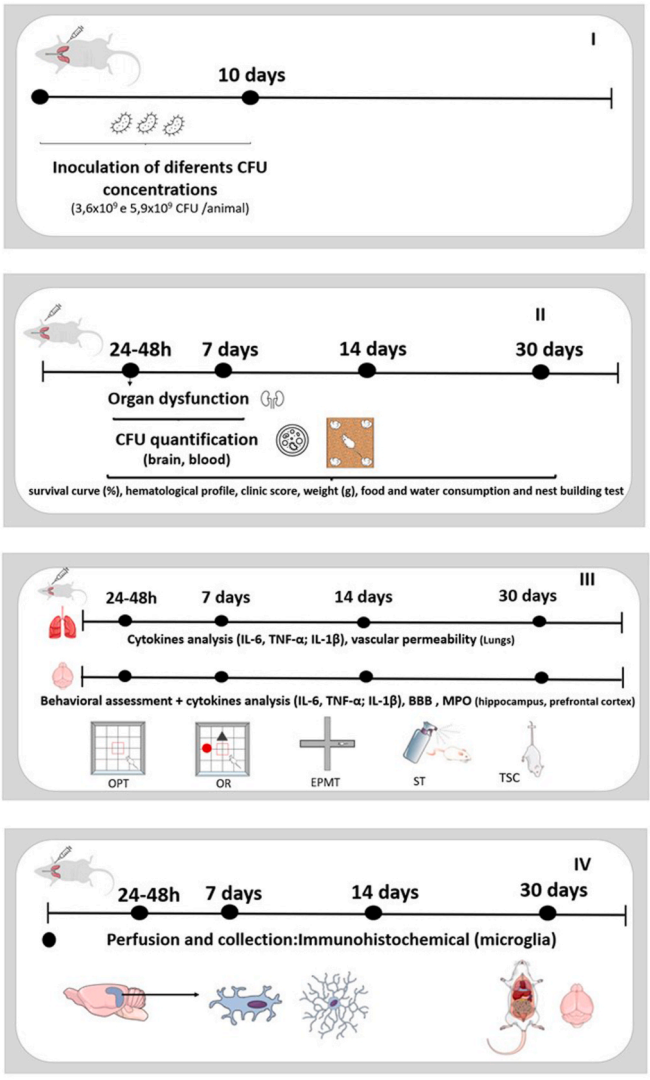

Fig. 1. Experimental protocols. Experiments I, II, III and IV. CFU: Colony Forming Units, MPO: myeloperoxidase, OPT: open field test, OR: object recognition, EPMT: elevated plus maze test, ST: sucrose test, TSC: tail suspension test. Source: Scheme planning of the figure of authorship, and illustration made using Mind the Graph, 2021.

2018). Thus, neurological disorders (e.g., encephalopathy, depression, anxiety, and cognitive disorders) are frequently reported in sepsis survivors (Hosokawa et al., 2014; Sharshar et al., 2014; Tsuruta and Oda, 2016). Also, sepsis can change consciousness, including mental confusion, torpor, and coma. For example, patients with sepsis-associated encephalopathy may develop mild delirium or even coma (Gofton and Young, 2012; Tsuruta and Oda, 2016). Sepsis-associated encephalopathy is also associated with an impaired prognosis and greater mortality (Russell et al., 2000; Schuler et al., 2018).

Central nervous system (CNS) dysfunction may occur during and after sepsis due to a systemic inflammatory response (Sonneville et al., 2013; Riel et al., 2015; Van der Poll et al., 2017; Denstaedt et al., 2020). Also, cytokine storm, chemokines release, and activation of peripheral immune cells may worsen brain damage (Van der Poll et al., 2017). The crosstalk between peripheral and central inflammation may lead to brain dysfunction and neurodegeneration; however, its mechanism is unclear (Salluh et al., 2010; Xin et al., 2023).

Although some studies have reported an association between lung infection and an increased risk of dementia, cognitive impairment, and differences in brain structures (Russ et al., 2020; Wang et al., 2022), its mechanisms need to be further investigated.

Table 1
Experimental protocols.

Experimental duration	Experimental description	Number of animals
Experiment I 10 days	A. Estimated the amount of colony-forming unit (CFU) of *Klebsiella pneumoniae*	n = 30
Experiment II 30 days	A. Quantified bacterial dissemination in blood and brain	n = 40
	B. Urea and creatinine measurements	n = 16
	C. Survival curve, clinical score, body weight (water and food intake) and animal well-being	n = 20
Experiment III 30 days	A. Behavioral assessments	
	Group 1	n = 20
	Group 2	n = 20
	Group 3	n = 20
	Group 4	n = 20
	B. Proinflammatory cytokines levels, vascular and blood-brain barrier (BBB) permeability, myeloperoxidase (MPO) activity in the lungs and brain	n = 64
Experiment IV 30 days	A. Microglial activation in the hippocampus using immunohistochemical analysis	n = 48

In this sense, this study aimed to investigate the relationship between lung inflammation, behavioral status, and cognitive function for up to 30 days in a model of pulmonary sepsis in mice. The hippocampal and prefrontal cortex inflammation and microglial activation were also assessed.

2. Methods

2.1. Animals and ethics statement

Male Swiss mice (n = 298) aged between six and eight weeks and weighing from 30 to 40 g were obtained from the animal facility of the Federal University of Santa Catarina (UFSC; Florianópolis, SC, Brazil). Three to five mice were placed in each cage under controlled conditions, with food and water *ad libitum*. In all experiments mice were randomly allocated to the control (i.e., false-inoculated) or sepsis group. Both groups were analyzed after 24–48h, 7, 14, and 30 days of sepsis induction. All procedures were approved by the research ethics committee of the UFSC (no. 8919250219) and followed the Animal Research: Reporting *In Vivo* Experiment (ARRIVE) guidelines (Kilkenny et al., 2010; Percie du Sert et al., 2020).

2.2. Experimental protocol

Four experimental protocols were sequentially performed (Fig. 1) and Table 1 (supplementary material). The experiment I (n = 30) estimated the exact amount of colony-forming unit (CFU) of *Klebsiella pneumoniae* using two concentrations based on previous studies (Sordi et al., 2013; Probst et al., 2019; Sumar et al., 2021). The concentrations of 3.6 x 10^9 and 5.9 × 10^9 CFU per mouse were tested. Mice were assessed every 24 h for ten days.

Experiment II (total n = 76) quantified bacterial dissemination in blood and brain after 24, 48, and 72 h and seven days of sepsis induction (n = 40). Urea and creatinine were also quantified in urine after 24 h to identify damage in distal organs (n = 16). Experiment II also included the analysis of a survival curve, clinical score, body weight (with water and food intake), and animal well-being 30 days after sepsis induction (n = 20).

Behavior tests were performed in experiment III (total n = 144) after 48 h and 7, 14, and 30 days of sepsis induction. Mice from different sepsis and control subgroups (four subgroups of 20 mice [n = 80]) were used to avoid habituation and possible bias. Proinflammatory cytokines levels, vascular and blood-brain barrier (BBB) permeability and

Table 2
– Clinical score.

Characteristics	Scores		Total
Appearance	0 = straight hair	1 = raised hair	
Aspects of the eyes	0 = normal	1 = with secretion	
Conscience	0 = alert	1 = drowsy	
Breathing	0 = normal fast	1 = slow laborious	
Activity	0 = active	1 = lethargic	2 = moribund

myeloperoxidase (MPO) activity in the lungs and brain were also assessed (four subgroups of 16 mice [n = 64]).

Experiment IV (n = 48) assessed microglial activation in the hippocampus using immunohistochemical analysis after 24 h and 7, 14, and 30 days of sepsis induction (n = 12 for each period). The experimental protocols are described in Table 1.

2.3. Model of pneumonia-induced sepsis (pulmonary sepsis)

Klebsiella pneumoniae (ATCC 700603; American Type Culture Collection, Rockville, USA) was inoculated in mice to induce pulmonary sepsis. Bacterial cultivation, pathogenicity, and quantification were previously described by Sordi et al. (2013). The concentration of 5.9 x 10^9 was selected for the subsequent experiments to represent sepsis in clinical reality, in which the mortality rate is between 40% and 65% (Rudd et al., 2020). Also, sepsis severity and systemic inflammation are associated with the inoculated concentration (Sordi et al., 2013; Gonçalves et al., 2017).

Mice were intraperitoneally anesthetized with ketamine and xylazine (0.04 and 0.1 mL/kg, respectively) and placed in a supine position of 45°. A vertical incision (5 mm) on the neck was performed under aseptic conditions, and 50 μL of bacterial suspension (sepsis group) or sterile phosphate-buffered saline (PBS; control group) was intratracheally injected using a sterile 30-gauge needle. After skin suture, mice received 30 mL/kg of sterile warm PBS subcutaneously for volume replacement (supplementary material). Mice were maintained at 37 °C in cages until anesthesia recovery and then housed in a temperature- and light-controlled room (22 ± 1 °C; 12 h light-dark cycle) with water and food *ad libitum*.

2.4. Assessment of body weight and food and water intake

Body weight and food and water intake were assessed for 30 days (every two days) using a digital scale (CK 1253, TM®, USA). The average food and water intake was calculated for each mouse, considering three to five mice per cage.

2.5. Clinical score

The sepsis morbidity was assessed for 30 days using a clinically adapted score (Machado et al., 2010; Gonçalves et al., 2017; Sumar et al., 2021). Further details are described in Table 2 (Supplementary Material).

2.6. Behavioral assessments

Behavioral tests were assessed after 48 h and 7, 14, 30 days of sepsis induction. All tests were performed during the daylight (9 a.m.–4 p.m.), at 23 °C, with humidity between 40% and 60%, and low-light intensity (12 lux). All apparatus were cleaned with 10% ethanol between tests. The tests were recorded (Logitech® camera) and evaluated by an evaluator blinded.

2.6.1. Open field test (OFT)

The OFT was used to assess locomotor and exploratory activities and anxiety-like behavior, such as thigmotaxis (i.e., tendency to remain close to walls) (Simon et al., 1994). In this test, mice were placed in the center of a square apparatus (40 cm wide, 60 cm deep, and 50 cm high) to explore the environment for 5 min. A camera was positioned at the top of the apparatus, and the evaluator left the room during the test. The total number of crossings, time (seconds) spent in the center of the apparatus, and percentage of crosses in the center were assessed (Prut and Belzung 2003).

2.6.2. Object recognition test (ORT)

An adapted ORT (Ennaceur et al., 1989) was used to assess short-term memory. Mice were placed in the apparatus for 5 min (as described in OFT) 24 h before the test (short habituation). On the test day, mice were placed in the apparatus to explore two identical objects (object A) for 5 min, then returned to the original cage (training phase). After 60 min, mice were placed again in the apparatus and exposed to one object A a new object (B) for another 5 min. Exploratory behavior was defined as smelling or touching the object with the nose, front paws, or both. A recognition index was calculated as (T novel × 100)/(T novel + T familiar), where T novel is the time spent exploring the new object (B) and T familiar is the time spent exploring object A.

2.6.3. Elevated plus maze (EPM) test

The EPM test was used to assess anxiety-like behavior, as proposed by Pellow et al. (1985). It evaluates the conflict between the innate fear of open areas and the instinct to explore new environments in mice (Rodgers and Dalvi, 1997).

The apparatus consists of a device elevated 60 cm from the floor, with two open arms (25 cm × 5 cm) and two closed arms (25 cm × 5 cm x 15 cm) on a central platform (5 cm × 5 cm). Mice were placed in the center of the apparatus facing a closed arm for 5 min. The experiment was recorded, and the number of entries in the open (OA) and closed arms was analyzed (defined by placing four paws into the arm area). The following formulas calculated the number of entries and time spent in the OA: percentage of entries in the OA = number of entries in the OA/total of entries x 100; and percentage of time in the OA = permanence (seconds) in OA/300 × 100. The number of entries in the closed arm was used to assess locomotor activity.

2.6.4. Sucrose splash test (SST)

The SST consists of applying a 10% sucrose solution on the dorsal face of the mice using a syringe, which makes the coat dirty and encourages grooming behavior. The latency (i.e., time between the sucrose application and beginning of grooming) and duration of the grooming were recorded for 5 min and used as an index of self-care and motivation; the lack of grooming is considered a depression-like behavior (Isingrini et al., 2010).

2.6.5. Tail suspension test (TST)

The TST was used to assess depression-like behavior. The groups were placed in visually isolated, noise-controlled apparatus. Each mouse was suspended and fixed to a bench 50 cm above the floor with adhesive tape on the tip of the tail. A camera in front of the mice recorded the test for 6 min. The latency and duration of the immobility (seconds) were assessed (Steru et al., 1985).

2.6.6. Nest building test

The nest building is an innate behavior in rodents (mainly for reproduction, maintaining body temperature, and escaping predators) and may indicate well-being (Gaskill et al., 2013). Approximately 1 h before the dark cycle, mice were placed individually in cages with a solid bottom and cotton tufts (four flakes of 2.5 g and 5 × 7 cm each) for nest build. After 12 h, each cage was photographed for a proper score, and the nest complexity was scored on a 5-point scale, as described by

Table 3
Nest building test.

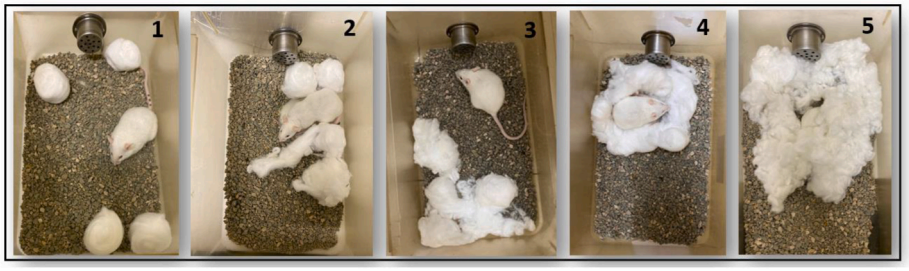

1.	The cotton remained untouched (>90% intact)
2.	The cotton has been partially shredded (approximately 50%–90% remains intact)
3.	The cotton was shredded (<50%), but the nest was not built
4.	A nest is built (>90% of shredded cotton), but the construction is still flat
5.	Nest formed, has "walls" that can completely cover the animal

Nest test. Nest construction assessment and score, which varies from 1 to 5.
In this experimental protocol, approximately 1 h before the start of the dark cycle, the animals were placed individually in boxes containing a solid bottom (odorless sanitary granules) and cotton tufts (4 flakes, 2.5 g each, measuring 5 × 7 cm) for the formation of nests (figure below). After 12 h, a photograph of each box was taken in order to calculate the score. In this way, the assessment of nest construction was considered over a period of 12 h, following the score (from 1 to 5) described above.

Deacon (2006). The scale is detailed in the Supplementary Material (Table 3).

2.7. Biochemical analyses

2.7.1. Quantification of bacterial dissemination

Bacterial dissemination was quantified in the brain and blood after 24, 48, and 72 h and seven days of sepsis induction. The blood and brain were collected, homogenized in 200 μL of PBS, and serially diluted in decimal factors. Next, 10 μL of each dilution (both samples) were placed on Mueller-Hinton agar plates at 37 °C. The number of CFU was counted, and results were expressed as log CFU.

2.7.2. Kidney function and hematological characteristics

Kidney function was assessed by quantifying urea and creatinine levels in urine using spectrophotometry 24 h after sepsis induction to represent damage to organs distal to the lungs. Mice were intraperitoneally anesthetized with ketamine and xylazine (0.04 and 0.1 mL/kg, respectively) and retro-orbital blood samples (0.5–1 mL) were obtained using Pasteur pipettes with the anticoagulant ethylenediaminetetraacetic acid (EDTA, Sigma, USA) and assessed (13 μL of each mouse) using an automatic hematology analyzer (Mindray™, Model BC-5300 vet, China).

2.7.3. Assessment of vascular and blood-brain barrier (BBB) permeability

The vascular permeability of lungs and BBB was assessed by determining the amount of extravasated Evans blue dye. Mice were lightly anesthetized with isoflurane and received Evans blue dye (40 mg/kg) in the retro-orbital plexus. After 30 min, mice were intraperitoneally anesthetized with ketamine and xylazine (0.04 and 0.1 mL/kg, respectively) and perfused with saline solution (0.9%) followed by 4% paraformaldehyde (PFA) used to clear blood and preserve brain for immunostaining according to Wu et al. (2021). Lungs, hippocampus, and prefrontal cortex were removed and weighed, and their pieces were incubated in 1 mL of aqueous formamide solution for 24 h at 55 °C. The optical density of the supernatant was read at 610 nm in a plate reader (Multi-reader TECAN™, USA), and results were interpolated using linear regression on a standard curve of Evans Blue dye. Data were expressed as μg/mg of tissue (Radu and Chernoff, 2013; Goldim et al., 2019).

2.7.4. MPO activity in lung and brain

Mice were intraperitoneally anesthetized with ketamine and xylazine (0.04 and 0.1 mL/kg, respectively). Lungs and brains were collected and placed in liquid nitrogen, and then tissues were transferred to PBS (20 mM, pH 7.4). The samples were centrifuged for 10 min at 13,000 G and 4 °C, and the supernatant was discarded. The pellet was resuspended in PBS (50 mM; pH 6.0) with hexadecyltrimethylammonium bromide (HTAB; 0.5%, w/v), the homogenate was centrifuged, and 30 μL of supernatant was used for enzyme analysis. The enzymatic reaction was conducted with tetramethylbenzidine (1.6 mM) and H_2O_2 (0.4 mM in 80 mM of PBS, pH 5.4), and the final concentration of H_2O_2 in the plate was 0.3 mM for lung and 3 mM for hippocampus and prefrontal cortex. The absorbance was measured in a plate reader (Ultra microplate reader EL 808, BiotTek Instruments™, USA) at 600 nm immediately after adding the H_2O_2 solution (for lungs) or after 4 min (for brain), with a final volume of 230 μL. The total protein concentration was estimated using bicinchoninic acid (BCA, Thermo Fischer Scientific™, Rockford, USA), and values were presented as optical density units/mg of total protein.

2.7.5. Cytokines assessment

Mice were intraperitoneally anesthetized with ketamine and xylazine (0.04 and 0.1 mL/kg, respectively). Lungs, hippocampus, and prefrontal cortex were collected and homogenized with PBS, Tween 20 (0.05%), phenylmethylsulphonyl fluoride (PMSF; 0.1 mM), EDTA (10 mM), aprotinin (2 ng/mL), and benzethonium chloride (0.1 mM) solution. Homogenates were transferred to Eppendorf tubes and centrifuged at 3000 rpm for 10 min at 4 °C, and the supernatants were stored at −80 °C until analyses. The level of tumor necrosis factor (TNF-α), interleukin-1β (IL-1β), and IL-6 were assessed using enzyme-linked immunosorbent assay (ELISA) according to manufacturer instructions (R&D Systems, Minneapolis, USA; ThermoFisher Scientific, USA). Cytokine levels were interpolated using linear regression on a standard curve of colorimetric measurements at 450 nm (correction wavelength 540 nm) in a plate reader (multi-reader, infinite m200 TECAN, USA). The total protein concentration (pg/mg) of the supernatant was measured using the Bradford method (Bradford, 1976), and all results were expressed as pg/mL of total cytokine.

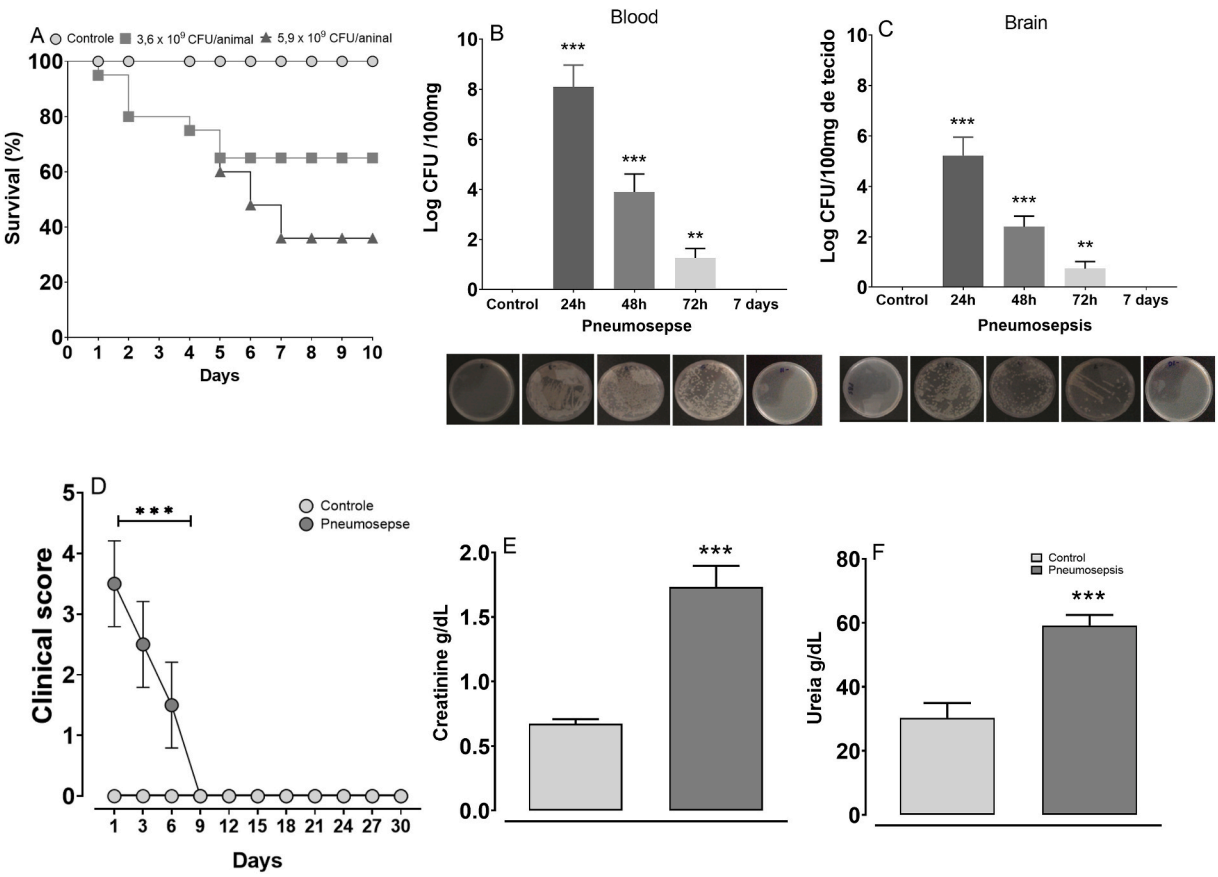

Fig. 2. (A): Survival curve: mice were inoculated intratracheally with 5.9 x 10^9 and 3.6 x 10^9 CFU/animal, control mice (false-inoculated) received saline (n = 10 animals/group). The results were expressed as a percentage of survival. Statistical analysis was performed using the log-rank test (Mantel Cox), *p < 0.01. The concentration of 5.9 x 109 CFU/animal was chosen for subsequent experiments. (B,C): Time course of bacterial spread in blood and brain: Blood and brain were collected, homogenized (brain) and diluted for growth on Mueller-Hinton agar plates. The data is expressed as log CFU, with n = 6 animals per group. Statistical analysis was performed using the Kruskal Wallis test, followed by the Dunn post-test. ***p < 0.001, ** <0.01; (D) Clinical score: animals in the control and pneumosepsis groups (n = 10/group) were scored on a scale ranging from 0 to 6 (indicating the best and worst clinical conditions, respectively) over a 30-day time course. Non-parametric analysis using the Kruskal Wallis test followed by Dunn post-test was conducted (***p < 0.001); (E and F): Renal dysfunction markers: creatinine (E) and urea (F) levels were measured 24 h after pneumosepsis in groups of 10 animals each. The results were analyzed using Student's t-test (p < 0.001). Values are expressed as mean ± SEM.

2.7.6. *Immunohistochemical study of hippocampus*

Mice were anesthetized intraperitoneally with ketamine (0.04 mL/kg) and xylazine (0.1 mL/kg), and cardiac perfusion was performed using 0.9% saline solution and 4% PFA to remove the brain, which was maintained in 4% PFA solution for 24–48 h (Gil-Mohapel et al., 2013; Pazini et al., 2017). Brain tissues were extracted and labeled with an ionized calcium-binding adapter protein-1 (IBA-1) antibody to assess the microglial activation in the hippocampus. The histological sections were washed three times with PBS (0.1 M) for 5 min. For antigenic recovery, two washes were performed with citrate buffer: one at room temperature for 5 min and the second at 50 °C in a water bath for 30 min. After three washes with 0.1 M PBS, sections were incubated in a peroxidase block solution containing 0.1 M PBS and 3% H_2O_2 (Merck™, Darmstadt, Germany). Next, they were washed three times with 0.1 M PBS and 0.3% Triton-X 100 buffer (Buffer, Sigma-Aldrich, Steinheim, Germany) and incubated in 2% bovine serum albumin solution (SigmaAldrich™, Steinheim, Germany) at room temperature for 1 h to block nonspecific reactions. Sections were incubated overnight with goat anti-IBA-1 antibody (Santa Cruz Biotechnology™, California, USA) at 4 °C. They were washed three times with buffer and then incubated for 2 h with rabbit anti-goat secondary antibody (1:500, Santa Cruz Biotechnology™, California, USA) biotinylated in a room temperature solution under constant stirring. After three washes with TA, sections were incubated with the avidin-biotin complex (ABC; Vector Laboratories™, California, USA) at room temperature for 2 h under constant stirring. Once the ABC was connected, three washes with 0.1 M PBS and two washes with acetate buffer were performed, and a 0.025% solution of 3, 3,9-hydrochloride of diaminobenzidine (DAB; Sigma-Aldrich™, Steinheim, Germany) was included with an 8% nickel solution in acetate buffer. Sections were washed once with acetate buffer and twice with 0.1 M PBS, and salinized slides were used for labeling. Slides were covered with Permount® (Fisher Scientific™, New Jersey, USA) and proper coverslips. Hippocampal images were obtained at 200x magnification (Image J Program, USA), and immunopositive areas were expressed as percentage of the total analyzed area. A blinded researcher analyzed the percentage of cells positive for IBA-1 in CA1, CA2, and CA3 areas of the hippocampus.

2.8. *Statistical analysis*

The Shapiro-Wilk test verified data normality. The *t*-test analyzed the kidney function, and the log rank (Mantel-Cox) test analyzed the survival curve. Body weight and food and water intake for 30 days were compared using the analysis of variance (ANOVA) for repeated measures with Tukey's post hoc test. The two-way ANOVA with Tukey's post hoc test was used for parametric data (behavioral tests, hematological characteristics, vascular and BBB permeability, MPO activity, cytokine levels, microglial activity) and Kruskal-Wallis with Dunn's post hoc test

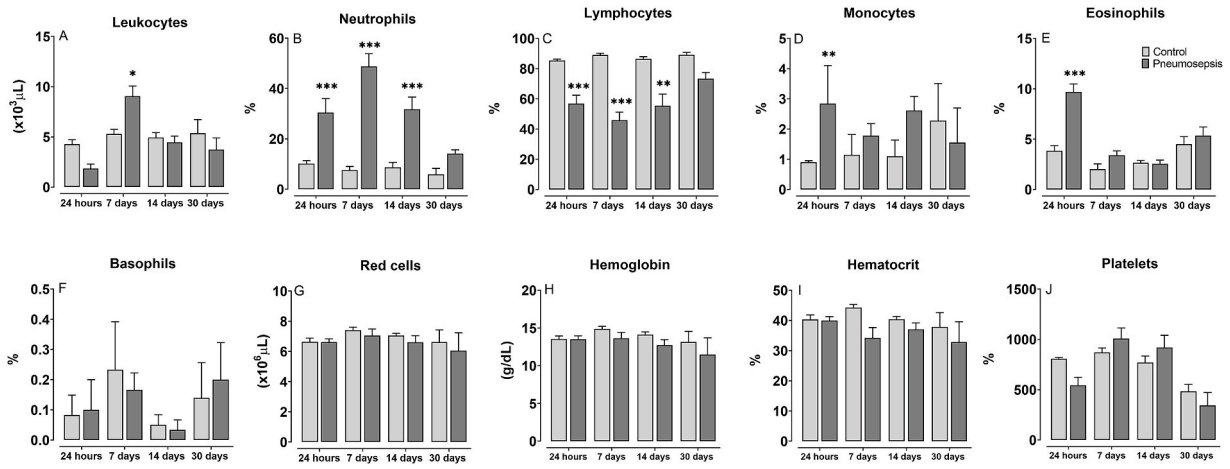

Fig. 3. Temporal hematological profile after pneumosepsis induction: (n = 6 animals/group). The data were analyzed by two-way ANOVA followed by Tukey's post-test. Significance levels were denoted as follows: *p < 0.05; **p < 0.01; ***p < 0.001). Values are expressed as mean ± SEM.

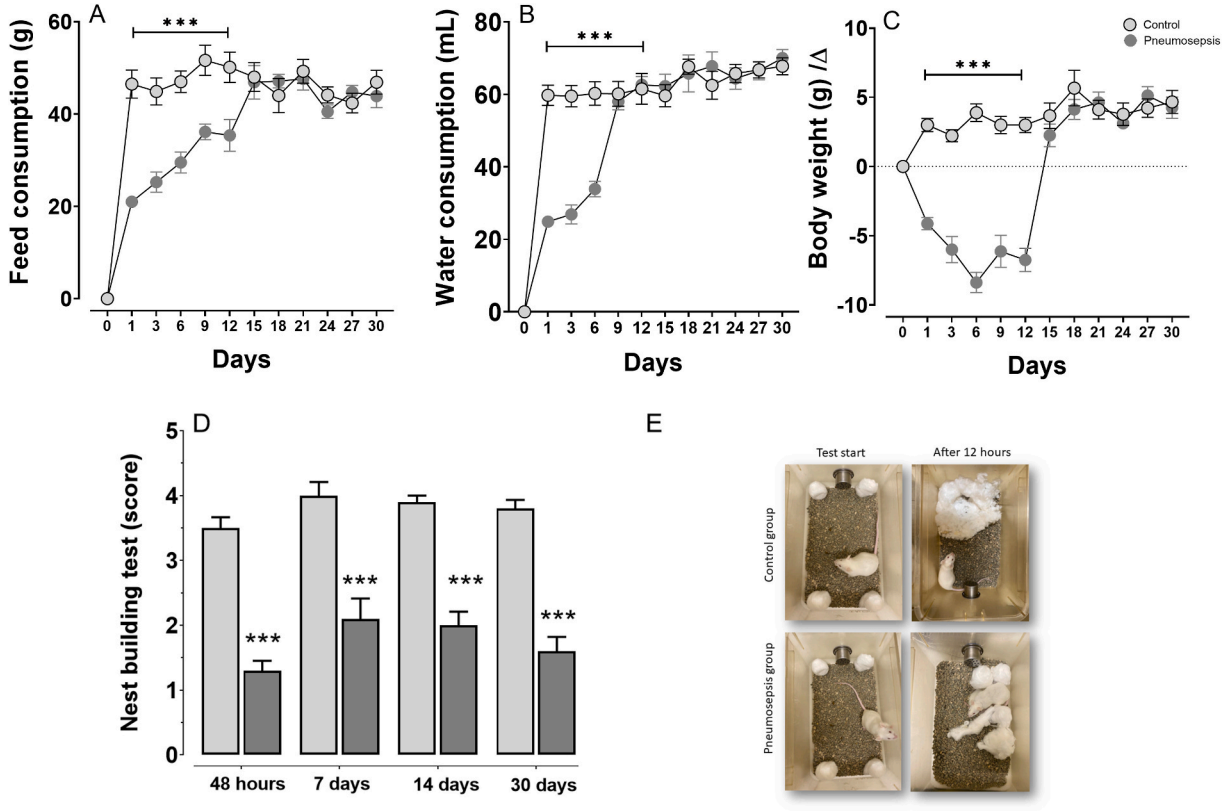

Fig. 4. (A and B) Feed and water consumption: The control and pneumosepsis groups were evaluated over a 30-day period. Repeated measures ANOVA followed by Tukey's post-test was performed. (***p < 0.001), (n = 10 animals/group).(C) Body weight assessment: The control and pneumosepsis groups were evaluated over a 30-day period. Repeated ANOVA followed by Tukey's post-test was performed (***p < 0.001), (n = 10 animals/group). (D) Nest test: scores were assigned based on parameters for nest formation (n = 10 animals/group). (E): Representation of a nest test result at 14 days, comparing control and pneumosepsis). Statistical analysis was performed using the Kruskal-Wallis test followed by Dunn post-test (***p < 0.001). Values are expressed as mean ± SEM.

for non-parametric data (bacterial dissemination, nest building test). Results were expressed as mean ± standard error of the mean or median and statistical significance was set at $p < 0.05$. All analyses and graphs were performed using the GraphPad Prism 8.0 (GraphPad Software®, San Diego, CA).

3. Results

3.1. Survival curve, clinical score, bacterial dissemination, hematological characteristics, and distal organ damage in mice with pulmonary sepsis

Concentrations of $3.6x10^9$ and 5.9×10^9 CFU resulted in mortality rates around 20% and 60% (respectively) after ten days of inoculation (Fig. 2A). Therefore, we selected the 5.9×10^9 CFU concentration of

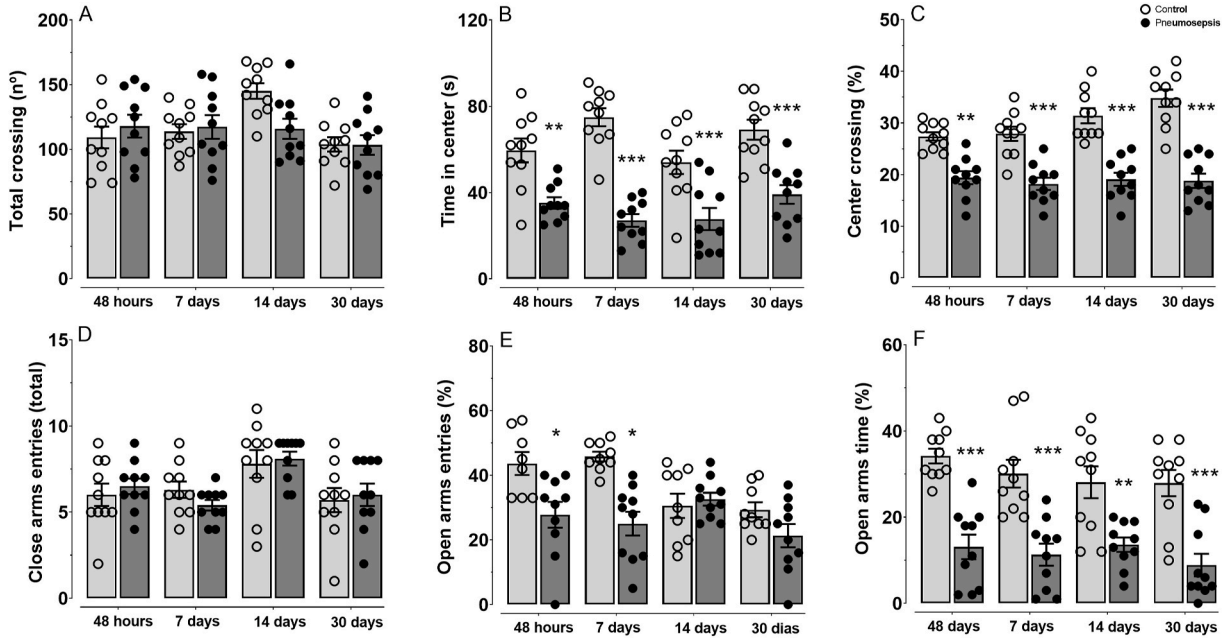

Fig. 5. Evaluation of behavioral parameters in the open field test: (A) Total number of crossings, (B) Time spent in the center of the apparatus (seconds), (C) Percentage of time spent in the center; in the maze test in raised cross: (D) Number of entries into closed arms, (E) Percentage of entries into open arms, (F) Percentage of time spent in the open arms. Each animal is represented by an individual symbol (n = 10 animals/group). Two-way ANOVA and Tukey's post-test were performed. (*p < 0.05, **p < 0.01 and ***p < 0.001). Values are expressed as mean ± SEM.

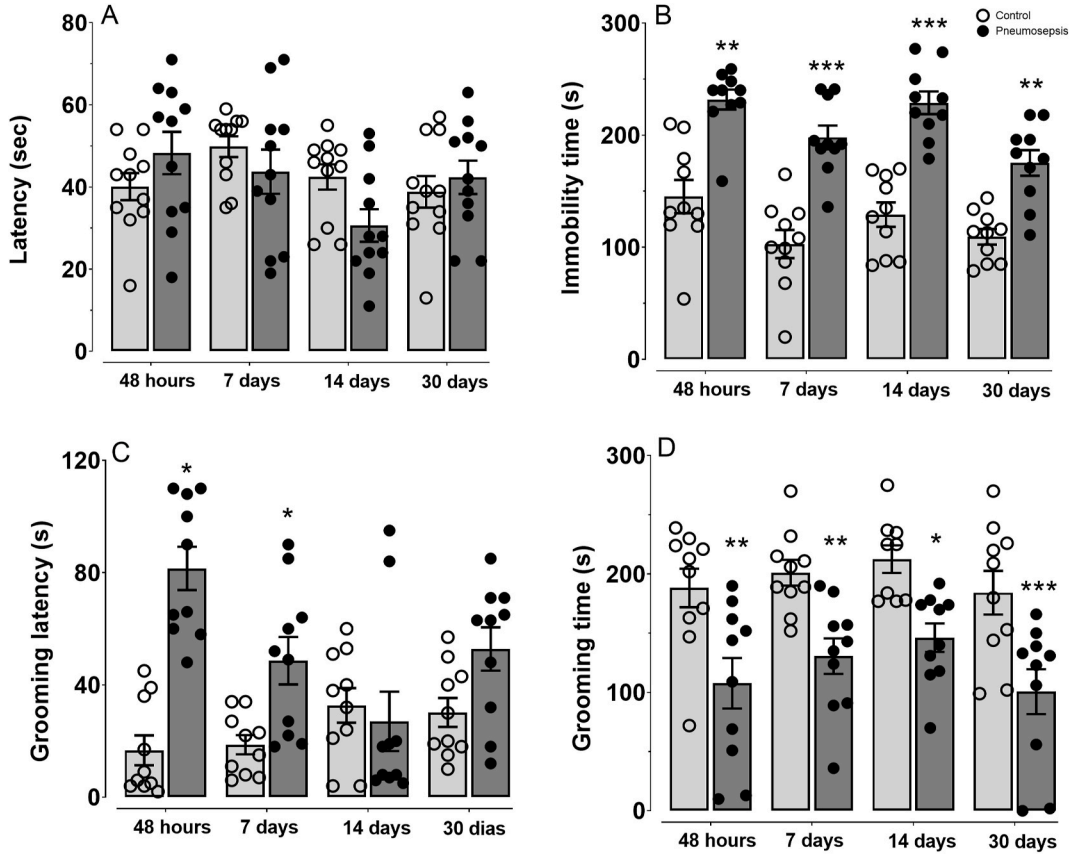

Fig. 6. Evaluation of behavioral parameters in the tail suspension test: (A) Latency to immobility, (B) Immobility time and in the sucrose spray test: (C) Latency for grooming and (D) Grooming time. Each animal is represented by an individual symbol (n = 10–12/group). Statistical analysis was performed using the two-way ANOVA test followed by Tukey's post-test (*p < 0.05, **p < 0.01, ***p < 0.001). The values are expressed as mean ± SEM.

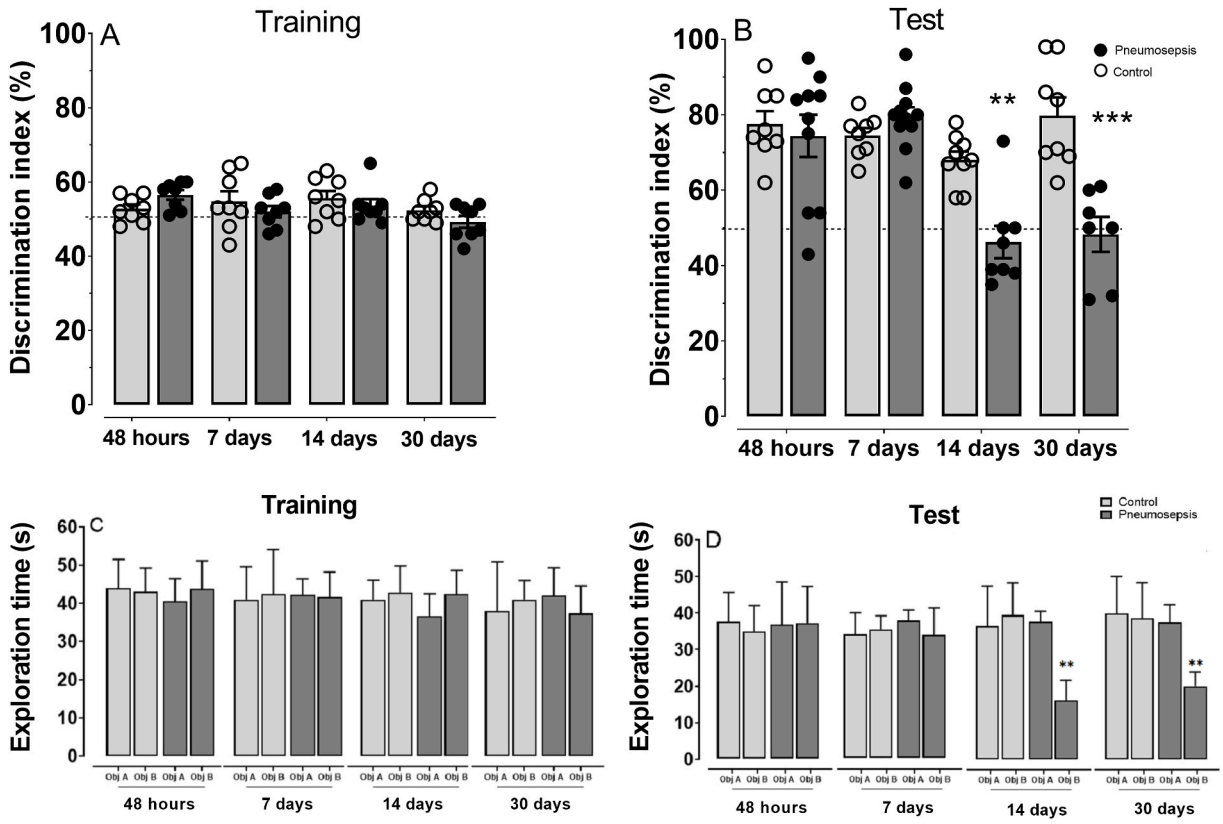

Fig. 7. Object Discrimination Index (A) Training and (B) Test; Exploration time (s) (C) Training and (D) Test. These evaluations were conducted using the object recognition test (short-term). Each animal is represented by an individual symbol (n = 8–10 animals/group). Statistical analysis was performed using the two-way ANOVA test followed by Tukey post-test (*p < 0.05, **p < 0.01, ***p < 0.001). Values are expressed as mean ± SEM.

Klebsiella pneumoniae for subsequent experiments. This concentration represented the clinical reality (about 60% mortality) and resulted in significant bacterial dissemination in blood (F [4,26] = 45.5; p > 0.001) (Fig. 2B) and brain (F [4,26] = 37.1; p > 0.001) (Fig. 2C) after 24 h (p < 0.001), 48 h (p < 0.001), and 72 h (p < 0.05). However, no bacterial dissemination was observed after seven days in blood (F [4,26] = 1.765; p = 0.187) and brain (F [4,26] = 0.234; p = 0.294).

Clinical score was increased in the sepsis group until the sixth day after induction compared with the control group (p < 0.001), which maintained clinical scores close to zero (Fig. 2D). Also, urea (t [6] = 5.615; p < 0.001) and creatinine levels (t [6] = 5.044; p < 0.001) increased in the first 24 h after sepsis induction (Fig. 2E and F), and white blood cell count increased (F [3,32] = 6.6; p < 0.01) until the seventh day (p < 0.01) (Fig. 3A). Significant neutrophilia (F [3,32] = 36.5; p < 0.001) and lymphocytopenia (F [3,32] = 90.4; p < 0.001) were also observed until the 14th day (Fig. 3B and C) and monocytes (F [3,32] = 9.85; p < 0.05) and eosinophils (F [3,32] = 23.62; p < 0.001) were increased in the first 24 h (Fig. 3D and E).

3.2. Sepsis group presented reduced water and food intake, significant weight loss, and reduced grooming behavior

A significant decrease in food (F [1,18] = 37.1; p > 0.001) (Fig. 4A) and water intake (F [1,18] = 39.24; p > 0.001) (Fig. 4B) and weight loss (F [1,18] = 33.04; p > 0.001) (Fig. 4C) were observed until the 12th day after sepsis induction. The overview of clinical conditions was also related to well-being since the sepsis group showed a lower score in the nest building test than the control group in all assessed periods (p < 0.001) (Fig. 4D and E).

3.3. Pulmonary sepsis induced anxiety- and depression-like behaviors and memory impairment in mice

The sepsis group showed no difference in the number of crossings in the OFT compared with the control group (F [3,72] = 2.59; p = 0.06) (Fig. 5A). However, sepsis decreased the time spent in the center of the OFT apparatus (F [3,72] = 73.24; p < 0.001) (Fig. 5B) after 48 (p < 0.05) and 7 (p < 0.001), 14 (p < 0.001), and 30 days (p < 0.001). The percentage of central crosses was also reduced in the sepsis group (F [3,72] = 11.12; p < 0.05) (Fig. 5C) after 48–72 h (p < 0.05) and 7 (p < 0.001), 14 (p < 0.001) and 30 days (p < 0.001). Although the total number of entries in the closed arms in the EPM test was not different between groups (F [3,72] = 0.65, p = 0.61) (Fig. 5D), sepsis group had an increase of percentage of entries in the OA (F [3,72] = 2.805; p < 0.04) after 48 h (p < 0.05) and 7 days (P < 0.05) (Fig. 5E). Also, the sepsis group had fewer entries in the OA than the control group after 48 (p = 0.01) and 7 days (p = 0.02) (Fig. 5F). No difference was observed between groups after 14 (p = 0.97) and 30 days (p = 0.86). Thus, data suggested an anxiety-like behavior in mice with pulmonary sepsis.

Although the sepsis group showed no differences in latency of immobility in the TST compared with the control group (F [3,72] = 2.53; p = 0.07) (Fig. 6A). The immobility duration was increased in the sepsis groups (F [3,72] = 8.13; p < 0.001) after 48 h (p < 0.001) and 7 (p < 0.001), 14 (p < 0.01), and 30 days of induction (p < 0.01) (Fig. 6B). In addition, the latency of grooming was increased in the sepsis groups (F [3,72] = 8.34; p < 0.001) after 48–72 h (p < 0.001) and seven days (p < 0.05) of induction (Fig. 6C) but not after 14 (p = 0.94) and 30 days (p = 0.26). The sepsis group had shorter duration of grooming than the control group after 48–72 h (p < 0.01) and 7 (p < 0.05), 14 (p < 0.05), and 30 days (p < 0. 05) (Fig. 6D). Thus, data from the TST and SST suggested that pulmonary sepsis induced depression-like behavior in mice.

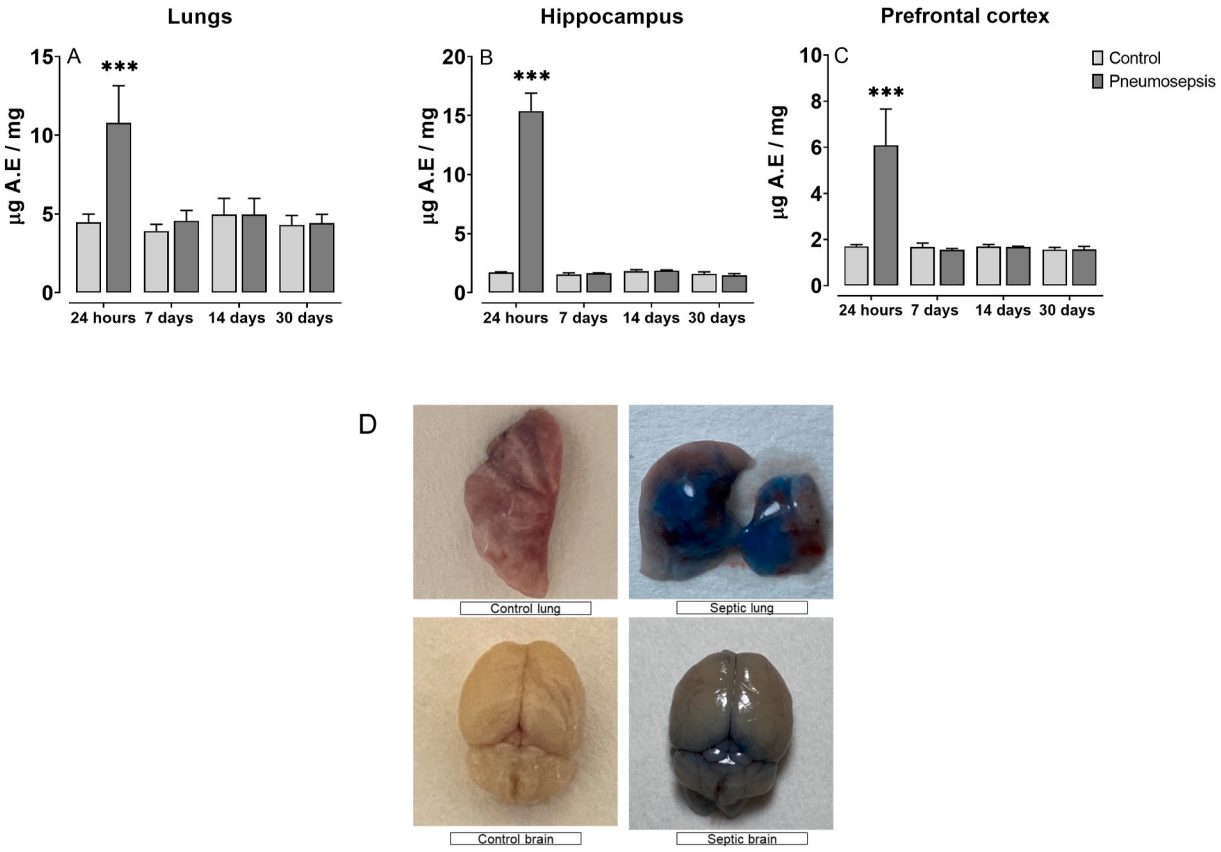

Fig. 8. Evaluation of tissue leakage using Evans Blue after pneumosepsis induction (n = 6 animals/group) in lungs (A), hippocampus (B) and prefrontal cortex (C). Data were analyzed by two-way ANOVA followed by Tukey's post-test. Significance levels were denoted as follows: *p < 0.05; **p < 0.01; ***p < 0.001). Values are expressed as mean ± SEM. Figure D demonstrates representative photos of tissues from the control group and pneumosepsis within 24 h after the induction of pneumosepsis.

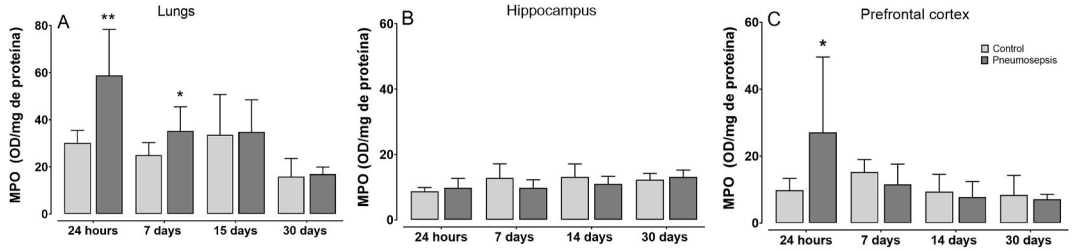

Fig. 9. MPO activity in lungs (A), hippocampus (B) and prefrontal cortex (C) after pneumosepsis induction (n = 6 animals/group). Data were analyzed by two-way ANOVA followed by Tukey's post-test. Significance levels were denoted as follows: *p < 0.05; **p < 0.01). Values are expressed as mean ± SEM.

ORT (Fig. 7A and B) showed no significant difference in the time spent exploring the two objects A in training, confirming no innate preference ($F [3,72] = 0.965$; $p = 0.856$). However, the sepsis group spent a shorter time exploring object B than object A ($F [3,72] = 6.548$; $p < 0.001$) after 14 and 30 days of induction ($p < 0.01$) (Fig. 7C and D), suggesting impaired memory in the sepsis group.

3.4. Pulmonary sepsis increased vascular and BBB permeability and cell migration in the lungs, hippocampus, and prefrontal cortex of mice

Sepsis group showed increased extravasation of Evans blue dye in the lung ($F [3,34] = 6.57$; $p < 0.001$) (Fig. 8A), hippocampus ($F [3,34] = 61.80$; $p < 0.001$) (Fig. 8B), and prefrontal cortex ($F [3,34] = 16.26$; $p < 0.001$) (Fig. 8C) 24h after sepsis induction, suggesting BBB increased vascular and permeability.

MPO activity was also increased in the lungs of the sepsis group ($F [3,40] = 10.87$; $p < 0.001$) (Fig. 9A) after 24 h ($p > 0.01$) and seven days ($p > 0.05$). Although this activity had no change in the hippocampus ($F [3,40] = 1.727$; $p = 0.174$) (Fig. 9B), it increased in the prefrontal cortex 24 h after sepsis induction ($F [3,40] = 3.55$; $p < 0.05$) (Fig. 9C).

3.5. Inflammatory cytokines were increased in the lung, hippocampus, and prefrontal cortex of mice with pulmonary sepsis

TNF-α levels were increased in the lungs ($F [3,56] = 63.67$; $p < 0.001$), hippocampus ($F [3,56] = 72.54$; $p < 0.001$), and prefrontal cortex ($F [3,56] = 45.59$; $p < 0.001$) of the sepsis group. It increased only at 24 h of sepsis induction in the lungs (Fig. 10A) but remained for 14 days in the hippocampus (Fig. 10B) and seven days in the prefrontal cortex (Fig. 10C). Simultaneously, IL-1β levels significantly increased in the lungs ($F [3,56] = 33.02$; $p < 0.001$) (Fig. 10D), prefrontal cortex ($F [3,56] = 46.13$; $p < 0.001$) (Fig. 10E), and hippocampus ($F [3,56] =$

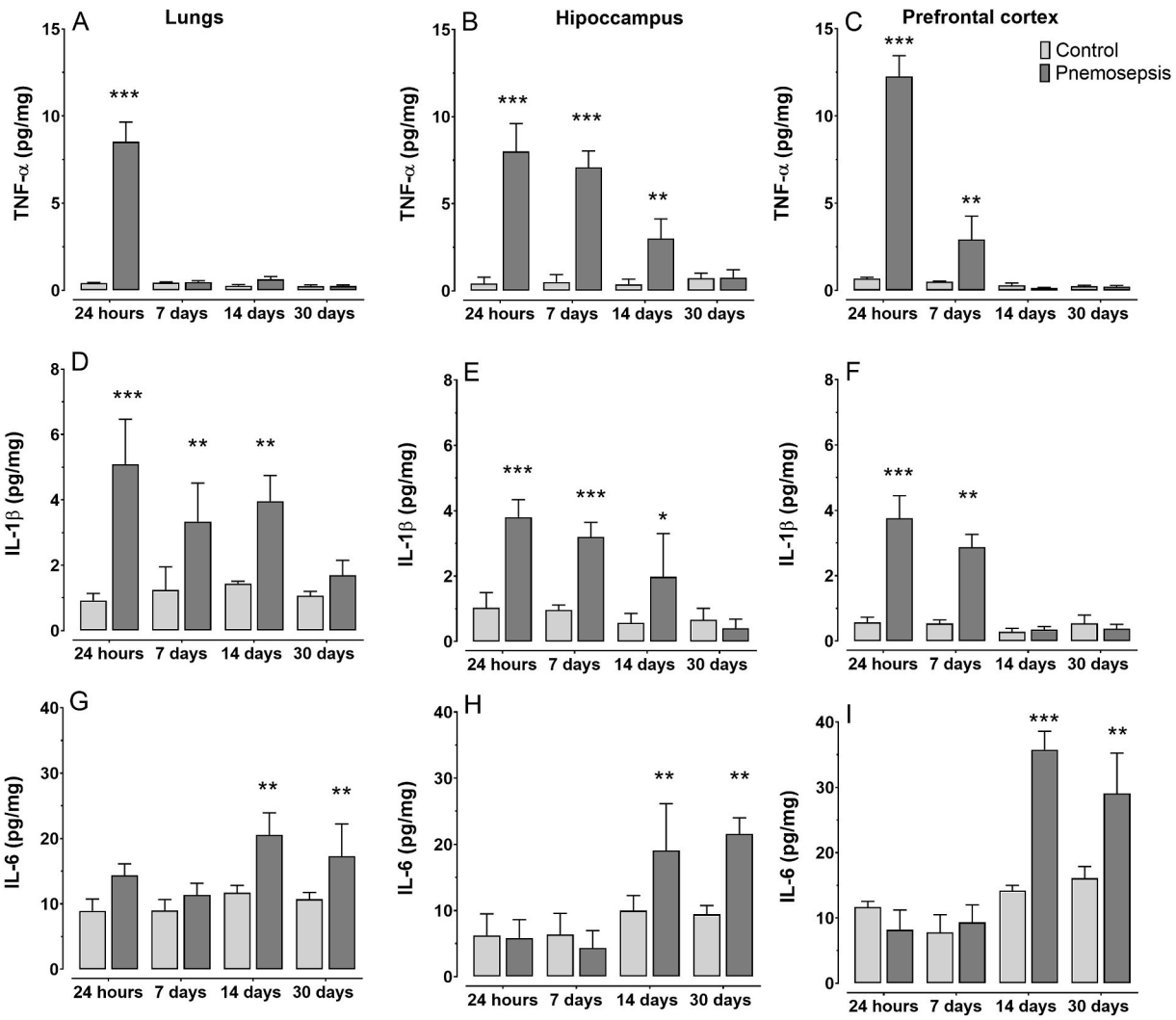

Fig. 10. Temporal profile of pro-inflammatory cytokines in the lungs, hippocampus and prefrontal cortex after induction of pneumosepsis (n = 8 animals/group). A, B, C: TNF-α concentration; D, E, F: IL-1β concentration; G, H, I: IL-6 concentration. Data were analyzed by two-way ANOVA followed by Tukey's post-test. Significance levels were denoted as follows: *p < 0.05; **p < 0.01; ***p < 0.001). Values are expressed as mean ± SEM.

30.61; p < 0.001) (Fig. 10F) for up to 14 days. In addition, IL-1β levels increased between 7 and 14 days after sepsis induction in the prefrontal cortex. A significant increase in IL-6 levels was also observed in the lungs (F [3,56] = 6.97; p < 0.01) (Fig. 10G), hippocampus (F [3,56] = 7.53; p < 0.01) (Fig. 10H), and prefrontal cortex (F [3,56] = 6.76; p < 0.001) (Fig. 10I) within 14 and 30 days after sepsis induction.

3.6. Microglial activation in the hippocampus of the sepsis group

Cells positive for IBA-1 were increased all over the hippocampus: CA1 (F [3,40] = 15.14; p < 0.001), CA2 (F [3,40] = 10.20; p < 0.001), and CA3 (F [3,40] = 19.34; p < 0.001) (Fig. 11A, B, and 11C, respectively). In addition, the percentage of positive cells in CA1 was increased in the sepsis group after 24 h (p > 0.01) and 7 (p > 0.05), 14 (p < 0.05), and 30 days (p < 0.05) of induction. However, cells positive for IBA-1 were increased only 24 h after sepsis induction (p < 0.001) in the CA2, and 24 h (p < 0.001), 7 (p < 0.01), and 14 days (p < 0.001) in the CA3 area.

Photomicrographs of cells positive for IBA-1 and with pathological findings of the sepsis group were compared with the control group (Fig. 12). Increased perivascular Virchow-Robin cells inside and outside the hippocampus and edema in the white matter were observed in the sepsis group. Also, a large area of cells positive for IBA-1 indicated a microglial activation in neuronal and perivascular areas in this group (see Fig. 13).

4. Discussion

This pulmonary sepsis model resulted in a systemic inflammatory response with brain damage, increased BBB permeability and proinflammatory cytokines levels in the CNS, neutrophil infiltration, and microglial activation in hippocampal areas. The anxiety- and depression-like behaviors and short-term cognitive impairment corroborated the biochemical and histological findings in the brain of sepsis survivor mice.

According to Alberti et al. (2002) and Sakr et al. (2018), *Klebsiella pneumoniae* is one of the main Gram-negative bacteria responsible for sepsis in hospitals. In this sense, our pulmonary sepsis model showed to be reproducible and standardized, with face, construct, and translational validity (Soares et al., 2006; Czaikoski et al., 2013; Prager et al., 2013; Sordi et al., 2013; Horewicz et al., 2015; Gonçalves et al., 2017; Probst et al., 2019). In addition, our data showed that an acute infection stimulated neuroinflammation, synapse damage, and neurodegeneration, resulting in neuropsychiatric disorders and cognitive impairments even after sepsis resolution, being in line with clinical studies (Iwashyna et al., 2010; Gao et al., 2017; Prescott and Angus

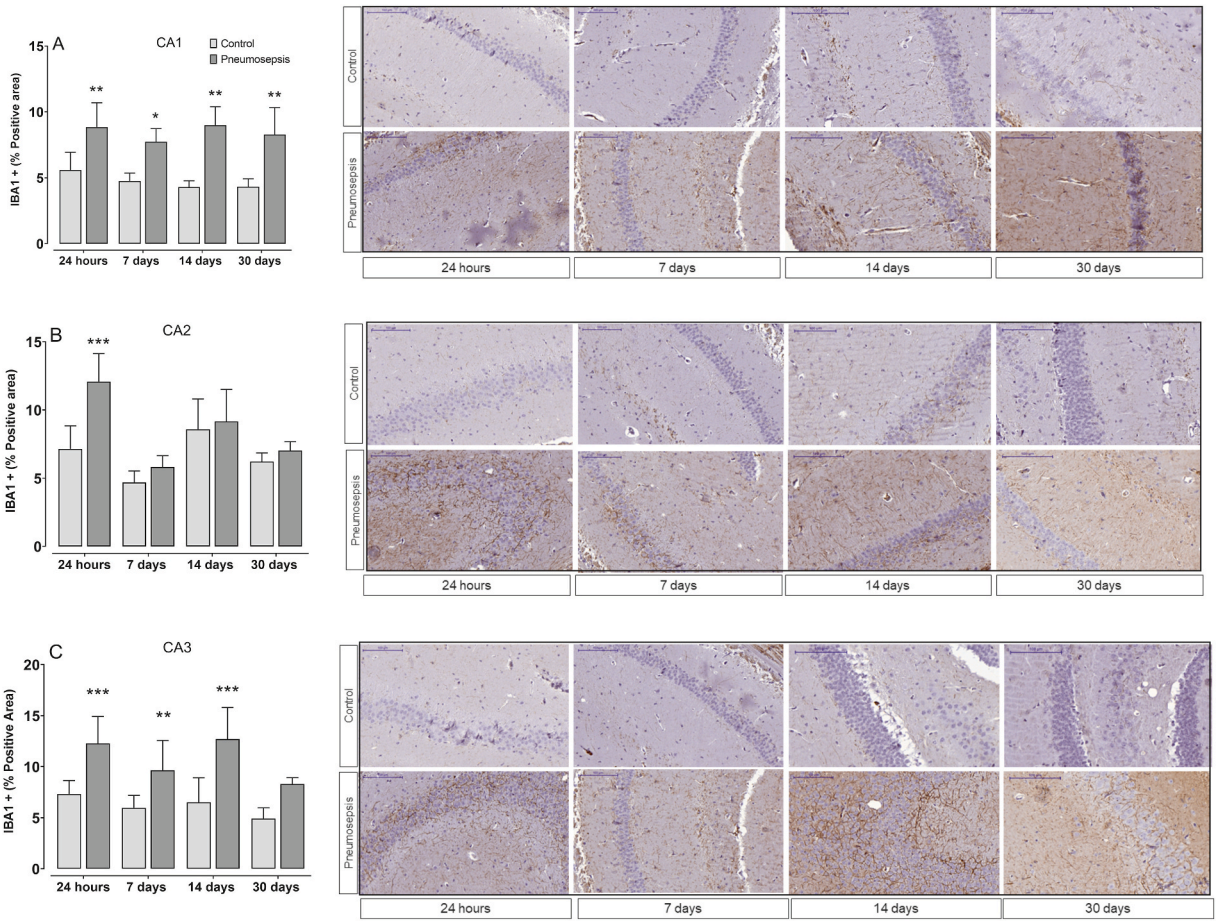

Fig. 11. Representative immunohistochemical panel of photomicrographs (increase of 200x) showing the percentage of area with cells positive for IBA1, a cellular marker of microglial activation, in the hippocampus (CA1, CA2 and CA3).
A: CA1 area, B: CA2 area, C: CA3 area. n = 6 animals/group. The data were analyzed by two-way ANOVA followed by Tukey's post-test. Significance levels were denoted as follows: *p < 0.05; **p < 0.01; ***p < 0.001). Values are expressed as mean ± SEM.

2018; Deanstaed et al., 2020; De Sousa et al., 2021).

In our study we also showed that mice recovered from pulmonary sepsis mainly from the 14th day, since they reestablished food and water intake and body weight, as well as improved the clinical score with no evidence of systemic bacterial dissemination. Thus, we performed behavior assessments from the 14th to 30th day after sepsis induction, assuming a full recovery from lung infection.

Despite biochemical, histological, and behavioral changes in the sepsis group, neuroinflammation was possibly unrelated to bacterial dissemination since we observed no evidence of chronic infection in the brain seven days after sepsis induction. Thus, it is plausible to hypothesing that a host immune response may be involved with both, the persistent neuroinflammation and behavioral changes, with a secondary inflammatory response induced by peripheral immune cells.

In this sense, the studies of Singer et al. (2016) partially corroborated with our hypothesis, by showing an association between the brain microbial exposure and neuroinflammation, but not a causative relationship between them, whether in post-mortem individuals as in an experimental model in mice.

In the other hand, some studies suggest that long-term neuroinflammation, persistent anxious and depressive behaviors and cognitive impairments may be related to systemic and inflammatory response, an important requirement for brain inflammation (Xin et al., 2023). Reinforcing this point of view, experimental and clinical researches have suggested that systemic immune activation outside the brain aggravates its damage in sepsis (Comim et al., 2011; Dal-Pizzol et al., 2013; Calsavara et al., 2013; Anderson et al., 2015; Gao et al., 2017; Goldim et al., 2020; D'Avila et al., 2018; Deanstaed et al., 2020; Dal-Pizzol et al., 2021; De Sousa et al., 2021; Kaukonen et al., 2014; Borges et al., 2015; Prescott and Angus, 2018). Nevertheless, these authors state the relationship between lung and brain dysfunction remains unclear.

In parallel, our study showed high levels of proinflammatory cytokines in lung, hippocampal and prefrontal cortex areas, as well as microglial activation in later stages of pulmonary sepsis induction.

In this regard, the early inflammatory response in sepsis is characterized by an excessive release of proinflammatory cytokines, resulting in multi-organ damage. The local inflammatory activation of innate immune cells in brain can also mediate its damage. Subsequently, peripheral immune cells are recruited before a large activation of brain endothelial cells and microglia to start secondary inflammatory responses (Van der Poll et al., 2017). Thus, proinflammatory mediators and chemokines (e.g., TNF-α, IL1-β, and IL-6) might intensify the microglial response and glial cell activation, exacerbating the neuroinflammation (Van der Poll et al., 2017), especially in the hippocampus, prefrontal cortex, and amygdala (Prager et al., 2013; Dal-pizzol et al., 2021).

In this study, we observed high levels of TNF and IL1-β in lungs and brain, followed by a later increase of IL-6 levels in both. These cytokines were increased at different time points, suggesting an independent production and release by resident cells, which contributed to both, lung and brain dysfunction. In this sense, localized inflammatory response syndrome may occur due to immunosuppression, contributing to bacterial entry, failure of phagocytosis and release of proinflammatory mediators (e.g., cytokines, nitric oxide, and proteolytic enzymes)

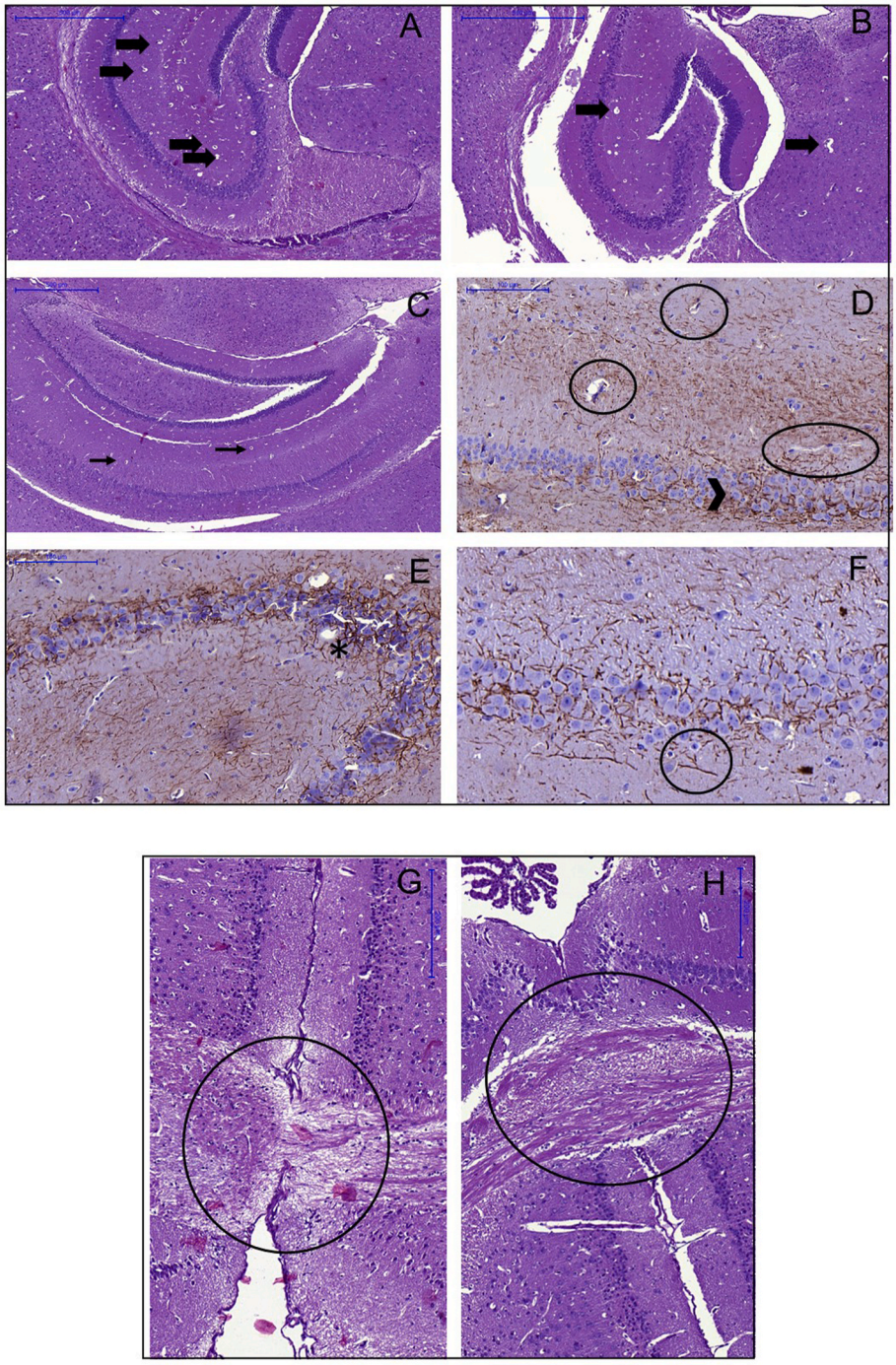

Fig. 12. A: Presence of enlarged Virchow-Robin perivascular spaces in animals with pneumosepsis (arrows); B: Enlarged perivascular spaces are often present in mice with pneumosepsis, within the hippocampus (arrow) and also outside it (arrow); C: Case control image of the hippocampus. It is observed that, in comparison with pneumosepsis cases, Virchow-Robin vascular spaces are inconspicuous (indicated by arrows); D: in mice with pneumosepsis, the microglial cells are not only present and permeating the hippocampal neuronal component (arrow) but also often found in perivascular regions (circles); E: Intensely branched microglia interspersing neuronal cells of the hippocampus in an animal with pneumosepsis (asterisk). F: individual microglial cell with processes marked by the immunopositivity for Iba-1; G: Photomicrograph of animal with pneumosepsis - loose/edematous stroma is observed in white substance of the corpus callosum (area circled in black). In the control animal, the corpus callosum is preserved, without significant histological changes.

(Gonçalves et al., 2017). Thus, in this experimental model, our results suggested that pulmonary inflammatory response may be involved in signaling anticipated the cytokine storm and cell recruitment in sepsis.

Septic mice showed increased BBB permeability in the hippocampus and prefrontal cortex and MPO activity in the prefrontal cortex 24 h after infection, with neutrophil infiltration, increasing brain damage in sepsis (Danielsky et al., 2018; Westhoff et al., 2019; Barichello et al., 2021). Additionally, our experimental model also resulted in leukocyte infiltration in the acute sepsis and sustained cytokine release (mainly of IL-6 levels) in brain and microglial activation in the CA1 area of the hippocampus during 30 days. Interestingly, these cellular and biochemical changes were followed by long-term behavioral changes.

IL-6 brain levels increased only in the recovery phase in sepsis in our study (i.e., 14th to 30th day). As it is known, IL-6 can increase vascular

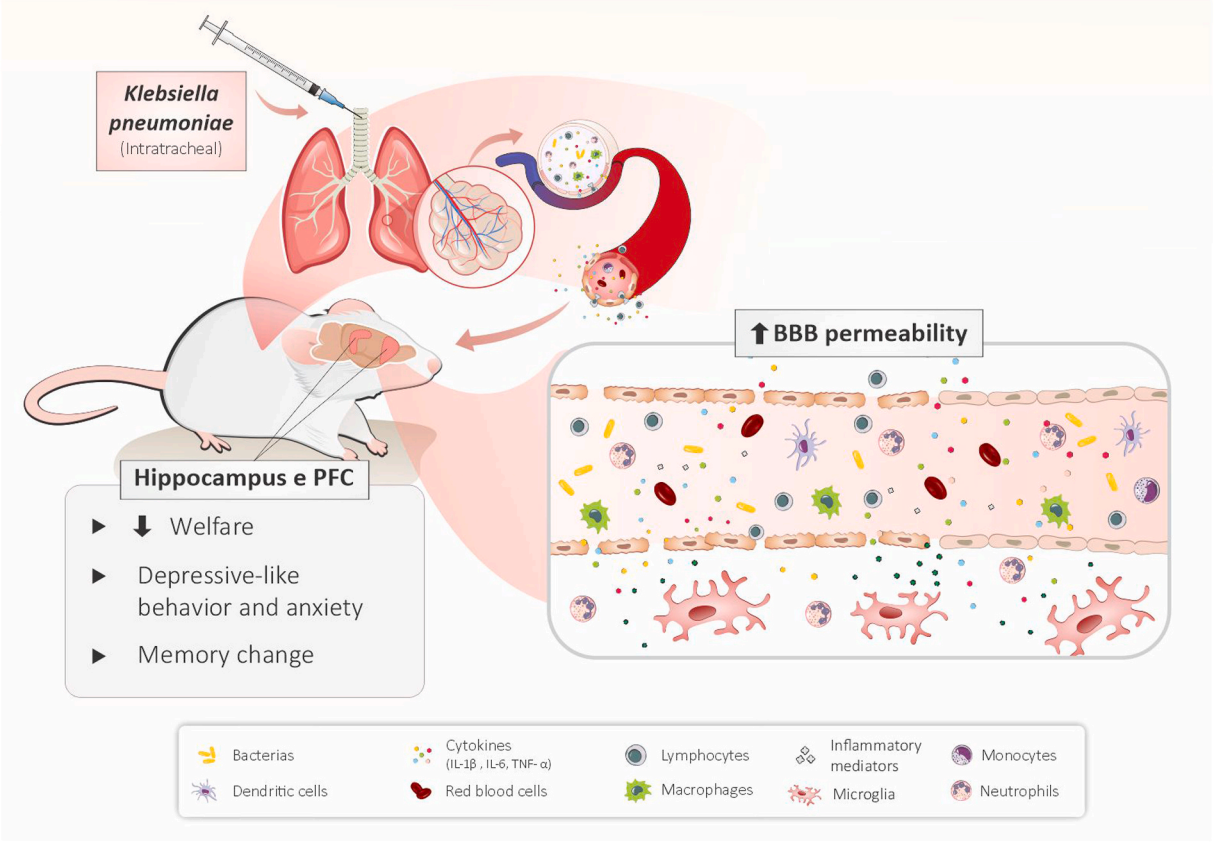

Fig. 13. Schematic representation of the main findings of the study. The model of pneumosepsis induced by instillation of *Klebsiella pneumoniae* can trigger systemic and neuroinflammatory responses, with behavioral repercussions, demonstrating an important translational approach. Source: Self-authored figure scheme planning, and illustration made by illustrator Priscila B. Rosa by CorelDraw and Mind the Graph, 2021.

permeability, facilitate lymphocyte activation and the antibody production, leading to CNS disorders (Richwine et al., 2008; Burton and Johnson, 2012; Hotchkiss et al., 2016; Venet and Monneret, 2017; Haileselassie et al., 2020; Willis et al., 2020). Thus, these data strengthen our hypothesis that proinflammatory cytokines affect brain function by crossing the BBB, resulting in cognitive impairments, behavioral changes, and decreased neurogenesis in the hippocampus.

These results corroborate with those showed by Mu-Huo et al. (2020), in an experimental study with rats exposed to lipopolysaccharide (LPS). LPS-group showed an increase in prefrontal cortex IL-6 levels, whereas rats treatment with minocycline (a microglial inhibitor) had IL-6 brain levels blunted, followed by an improvement of cognitive function, suggesting the involvement and influence of IL-6 on cognitive function (Mu-Huo et al., 2020).

In the TST, septic mice showed increased immobility duration in all assessed periods, demonstrating passive behavior before an acute stressful situation (Steru et al., 1985; Commons et al., 2017). They also showed decreased grooming duration during the SST, suggesting decreased motivation and increased anhedonic-like behavior (Pizzagalli, 2014; Planchez et al., 2019). In addition, the sepsis group remained in the closed arms of the EPM for a longer period and in the center of the OFT for a shorter period, suggesting a lack of exploratory and an anxiety-like behavior.

In this sense, biochemical and cellular theories were described to relate behavioral changes and sepsis. One theory is regarding the increase of BBB permeability, which may facilitate cell and cytokines entry and peripheral immune responses in the CNS, triggering or exacerbating microglial activation (Comim et al., 2011; Danielski et al., 2018; Westhoff et al., 2019; Barichello et al., 2021). Although the involvement of the BBB in neuroinflammation and behavioral changes in animals, the increase in permeability and changes in endothelial junctions may occur briefly and acutely (Westhoff et al., 2019; Barichello et al., 2021). However, persistent neuroinflammation was considered a mechanism for chronic brain dysfunction in sepsis survivors since high levels of inflammatory mediators were related to depressive disorders, anxiety, fatigue, and decreased quality of life (Prescott and Angus, 2018). Interestingly, our results showed not only an increase of BBB permeability in sepsis group, - observed by the amount of Evans blue dye extravasation in hippocampus and prefrontal cortex right after sepsis induction -, but also an activation of cells brain and a local increase of proinflammatory cytokines.

Some studies suggested that microglial activation in the hippocampus leads to a less robust interaction between astrocytes and neuronal units, resulting in lower maintenance of neuronal synapses (Azevedo et al., 2013; De Sousa et al., 2021). Also, it may increase microglial phagocytic capacity in synapses and even neuronal death, which may be related to cognitive and behavioral disorders (Azevedo et al., 2013; Moraes et al., 2015; Barichello et al., 2021; De Sousa et al., 2021), just like we observed, which corroborated to previous studies (Anderson et al., 2015; Gao et al., 2017; Michels et al., 2020).

In conclusion, this experimental pulmonary sepsis model in mice showed one of several aspects of sepsis and induced depression and anxiety-like behaviors, memory impairments and neuroinflammatory responses in the hippocampus and prefrontal cortex. Therefore, in this experimental model, we approached many sepsis aspects, like behavioral disorders, biochemical changes and histopathological aspects of brain, pointing out the lung-brain crosstalk in septic survivor mice.

CRediT authorship contribution statement

Kelly Cattelan Bonorino: Writing – review & editing, Writing – original draft, Visualization, Supervision, Resources, Project administration, Methodology, Investigation, Formal analysis, Data curation, Conceptualization. **Scheila Iria Kraus:** Writing – original draft, Resources, Methodology, Investigation, Formal analysis, Data curation. **Gisele Henrique Cardoso Martins:** Resources, Methodology, Investigation, Data curation. **Jéssica Jorge Probst:** Resources, Methodology, Investigation, Data curation. **Débora Melissa Petry Moeke:** Resources, Methodology, Investigation, Data curation. **Alice Henrique dos Santos Sumar:** Methodology, Investigation, Formal analysis. **Yuri Reis Casal:** Resources, Methodology, Investigation, Formal analysis. **Filipe Rodolfo Moreira Borges Oliveira:** Resources, Methodology, Investigation, Formal analysis. **Regina Sordi:** Visualization, Supervision, Methodology, Formal analysis. **Jamil Assreuy:** Supervision, Project administration, Methodology, Investigation, Funding acquisition, Conceptualization. **Morgana Duarte da Silva:** Writing – review & editing, Writing – original draft, Supervision, Methodology, Investigation, Formal analysis, Data curation. **Deborah de Camargo Hizume Kunzler:** Writing – review & editing, Writing – original draft, Visualization, Supervision, Project administration, Methodology, Investigation, Funding acquisition, Formal analysis, Data curation, Conceptualization.

Declaration of competing interest

The authors declare the following financial interests/personal relationships which may be considered as potential competing interests:

Jamil Assrey reports financial support, equipment, drugs, or supplies, and writing assistance were provided by INCT-INOVAMED. If there are other authors, they declare that they have no known competing financial interests or personal relationships that could have appeared to influence the work reported in this paper.

Data availability

The authors are unable or have chosen not to specify which data has been used.

Acknowledgments

This article is dedicated to the memory of Prof. Ph.D. Adair Roberto Soares dos Santos. We are immensely grateful to Prof. Adair, a great friend and mentor who contributed intensely to our study (concept, research design, and providing facilities) and recently passed away, being deeply missed. We also thank the Post-Graduate Program of Neurosciences of the UFSC, Multiuser Laboratory of Biology Studies (LAMEB/UFSC), and the Center for Innovation and Pre-Clinical Trials (CIEnP) for supporting the experiments. This study was financed in part by the Programa INCT-INOVAMED (grant no. 465430/2014-7), Fundação de Amparo à Pesquisa e Inovação do Estado de Santa Catarina (FAPESC), Conselho Nacional de Desenvolvimento Científico e Tecnológico (CNPq), and Coordenação de Aperfeiçoamento de Pessoal de Nível Superior (CAPES) - finance code 001.

Appendix A. Supplementary data

Supplementary data to this article can be found online at https://doi.org/10.1016/j.bbih.2024.100823.

References

Adhikari, N.K., Fowler, R.A., Bhagwanjee, S., Rubenfeld, G.D., 2010. Critical care and the global burden of critical illness in adults. Lancet 376 (9749), 1339–1346. https://doi.org/10.1016/S0140-6736(10)60446-1.

Alberti, C., Brun-Buisson, C., Burchardi, H., Martin, C., Goodman, S., Artigas, A., Sicignano, A., Palazzo, M., Moreno, R., Boulmé, R., Lepage, E., Le Gall, R., 2002. Epidemiology of sepsis and infection in ICU patients from an international multicentre cohort study. Intensive Care Med. 28 (2), 108–121. https://doi.org/10.1007/s00134-001-1143-z.

Anderson, S.T., Commins, S., Moynagh, P.N., Coogan, A.N., 2015. Lipopolysaccharide-induced sepsis induces long-lasting affective changes in the mouse. Brain Behav. Immun. 43, 98–109. https://doi.org/10.1016/j.bbi.2014.07.007.

Azevedo, E.P., Ledo, J.H., Barbosa, G., Sobrinho, M., Diniz, L., Fonseca, A.C., Gomes, F., Romão, L., Lima, F.R., Palhano, F.L., Ferreira, S.T., Foguel, D., 2013. Activated microglia mediate synapse loss and short-term memory deficits in a mouse model of transthyretin-related oculoleptomeningeal amyloidosis. Cell Death Dis. 4, e789 https://doi.org/10.1038/cddis.2013.325.

Barichello, T., Generoso, J.S., Collodel, A., Petronilho, F., Dal-Pizzol, F., 2021. The blood-brain barrier dysfunction in sepsis. Tissue Barriers 9 (1), 1840912. https://doi.org/10.1080/21688370.2020.1840912.

Borges, R.C., Carvalho, C.R., Colombo, A.S., da Silva Borges, M.P., Soriano, F.G., 2015. Physical activity, muscle strength, and exercise capacity 3 months after severe sepsis and septic shock. Intensive Care Med. 41 (8), 1433–1444. https://doi.org/10.1007/s00134-015-3914-y.

Bradford, M.M., 1976. A rapid and sensitive method for the quantitation of microgram quantities of protein utilizing the principle of protein-dye binding. Anal. Biochem. 7 (72), 248–254. https://doi.org/10.1006/abio.1976.9999.

Burton, M.D., Johnson, R.W., 2012. Interleukin-6 trans-signaling in the senescent mouse brain is involved in infection-related deficits in contextual fear conditioning. Brain Behav. Immun. 26 (5), 732–738. https://doi.org/10.1016/j.bbi.2011.10.008.

Calsavara, A.C., Rodrigues, D.H., Miranda, A.S., Costa, P.A., Lima, C.X., Vilela, M.C., Rachid, M.A., Teixeira, A.L., 2013. Late Anxiety-like behavior and neuroinflammation in mice subjected to sublethal polymicrobial sepsis. Neurotox. Res. 24 (2), 103–108. https://doi.org/10.1007/s12640-012-9364-1.

Comim, C.M., Vilela, M.C., Constantino, L.S., Petronilho, F., Vuolo, F., Lacerda-Queiroz, N., Rodrigues, D.H., da Rocha, J.L., Teixeira, A.L., Quevedo, J., Dal-Pizzol, F., 2011. Traffic of leukocytes and cytokine upregulation in the central nervous system in sepsis. Intensive Care Med. 37 (4), 711–718. https://doi.org/10.1007/s00134-011-2151-2.

Commons, K.G., Beck, S.G., Beyeler, A., Dong, Y., Mears, D., Ricci, L.A., Li, Y., 2017. The Rodent forced swim test measures stress-coping strategy, not depression-like behavior. ACS Chem. Neurosci. 8 (5), 955–960. https://doi.org/10.1021/acschemneuro.7b00042.

Czaikoski, P.G., Nascimento, D.C., Sônego, F., de Freitas, A., Turato, W.M., de Carvalho, M.A., Santos, R.S., de Oliveira, G.P., dos Santos Samary, C., Tefe-Silva, C., Alves-Filho, J.C., Ferreira, S.H., Rossi, M.A., Rocco, P.R., Spiller, F., Cunha, F.Q., 2013. Heme oxygenase inhibition enhances neutrophil migration into the bronchoalveolar spaces and improves the outcome of murine pneumonia-induced sepsis. Shock 39 (4), 389–396. https://doi.org/10.1097/SHK.0b013e31828bbcf9.

D'Avila, J.C., Siqueira, L.D., Mazeraud, A., Azevedo, E.P., Foguel, D., Castro-Faria-Neto, H.C., Sharshar, T., Chrétien, F., Bozza, F.A., 2018. Aged-related cognitive impairment is associated with long-term neuroinflammation and oxidative stress in a mouse model of episodic systemic inflammation. J. Neuroinflammation 15 (1), 28. https://doi.org/10.1186/s12974-018-1059-y.

Dal-Pizzol, F., Rojas, H.A., dos Santos, E.M., Vuolo, F., Constantino, L., Feier, G., Pasquali, M., Comim, C.M., Petronilho, F., Gelain, D.P., Quevedo, J., Moreira, J.C., Ritter, C., 2013. Matrix metalloproteinase-2 and metalloproteinase-9 activities are associated with blood-brain barrier dysfunction in an animal model of severe sepsis. Mol. Neurobiol. 48 (1), 62–70. https://doi.org/10.1007/s12035-013-8433-7.

Dal-Pizzol, F., de Medeiros, G.F., Michels, M., Mazeraud, A., Bozza, F.A., Ritter, C., Sharshar, T., 2021. What animal models can tell us about long-term psychiatric symptoms in sepsis survivors: a systematic review. Neurotherapeutics 18 (2), 1393–1413. https://doi.org/10.1007/s13311-020-00981-9.

Danielski, L.G., Giustina, A.D., Badawy, M., Barichello, T., Quevedo, J., Dal-Pizzol, F., Petronilho, F., 2018. Brain barrier breakdown as a cause and consequence of neuroinflammation in sepsis. Mol. Neurobiol. 55 (2), 1045–1053. https://doi.org/10.1007/s12035-016-0356-7.

De Sousa, V.L., Araújo, S.B., Antonio, L.M., Silva-Queiroz, M., Colodeti, L.C., Soares, C., Barros-Aragão, F., Mota-Araujo, H.P., Alves, V.S., Coutinho-Silva, R., Savio, L.E.B., Ferreira, S.T., Da Costa, R., Clarke, J.R., Figueiredo, C.P., 2021. Innate immune memory mediates increased susceptibility to Alzheimer's disease-like pathology in sepsis surviving mice. Brain Behav. Immun. 95, 287–298. https://doi.org/10.1016/j.bbi.2021.04.001.

Deacon, R.M., 2006. Assessing nest building in mice. Nat. Protoc. 1 (3), 1117–1119. https://doi.org/10.1038/nprot.2006.170.

Denstaedt, S.J., Spencer-Segal, J.L., Newstead, M., Laborc, K., Zeng, X., Standiford, T.J., Singer, B.H., 2020. Persistent neuroinflammation and brain-specific immune priming in a novel survival model of murine pneumosepsis. Shock 54 (1), 78–86. https://doi.org/10.1097/SHK.0000000000001435.

Ennaceur, A., Cavoy, A., Costa, J.C., Delacour, J., 1989. A new one-trial test for neurobiological studies of memory in rats. II: effects of piracetam and pramiracetam. Behav. Brain Res. 33 (2), 197–207. https://doi.org/10.1016/s0166-4328(89)80051-8.

Evans, L., Rhodes, A., Alhazzani, W., Antonelli, M., Coopersmith, C.M., French, C., et al., 2021. Surviving sepsis campaign: international guidelines for management of sepsis and septic shock 2021. Intensive Care Med. 47 (11), 1181–1247. https://doi.org/10.1007/s00134-021-06506-y.

Fleischmann, C., Scherag, A., Adhikari, N.K., Hartog, C.S., Tsaganos, T., Schlattmann, P., Angus, D.C., Reinhart, K., 2016. International forum of acute care trialists. Assessment of global incidence and mortality of hospital-treated sepsis. Current estimates and limitations. Am. J. Respir. Crit. Care Med. 193 (3), 259–272. https://doi.org/10.1164/rccm.201504-0781OC.

Gao, R., Ji, M.H., Gao, D.P., Yang, R.H., Zhang, S.G., Yang, J.J., Shen, J.C., 2017. Neuroinflammation-induced downregulation of hippocampal neuregulin 1-ErbB4 signaling in the parvalbumin interneurons might contribute to cognitive impairment in a mouse model of sepsis-associated encephalopathy. Inflammation 40 (2), 387–400. https://doi.org/10.1007/s10753-016-0484-2.

Gaskill, B.N., Karas, A.Z., Garner, J.P., Pritchett-Corning, K.R., 2013. Nest building as an indicator of health and welfare in laboratory mice. JoVE (82), 51012. https://doi.org/10.3791/51012.

Gil-Mohapel, J., Brocardo, P.S., Choquette, W., Gothard, R., Simpson, J.M., Christie, B.R., 2013. Hippocampal neurogenesis levels predict WATERMAZE search strategies in the aging brain. PLoS One 8 (9), e75125. https://doi.org/10.1371/journal.pone.0075125.

Gofton, T.E., Young, G.B., 2012. Sepsis-associated encephalopathy. Nat. Rev. Neurol. 8 (10), 557–566. https://doi.org/10.1038/nrneurol.2012.183.

Goldim, M.P.S., Della Giustina, A., Petronilho, F., 2019. Using Evans blue dye to determine blood-brain barrier integrity in rodents. Curr. Protoc. Im. 126 (1), e83 https://doi.org/10.1002/cpim.83.

Goldim, M.P.S., Della Giustina, A., Mathias, K., de Oliveira Junior, A., Fileti, M.E., De Carli, R., et al., 2020. Sickness behavior score is associated with neuroinflammation and late behavioral changes in polymicrobial sepsis animal models. Inflammation 43 (3), 1019–1034. https://doi.org/10.1007/s10753-020-01187-z.

Gonçalves, M.C., Horewicz, V.V., Lückemeyer, D.D., Prudente, A.S., Assreuy, J., 2017. Experimental sepsis severity score associated to mortality and bacterial spreading is related to bacterial load and inflammatory profile of different tissues. Inflammation 40 (5), 1553–1565. https://doi.org/10.1007/s10753-017-0596-3.

Gül, F., Arslantaş, M.K., Cinel, İ., Kumar, A., 2017. Changing definitions of sepsis. Turkish J. Anesthesiol. Reanim. 45 (3), 129–138. https://doi.org/10.5152/TJAR.2017.93753.

Haileselassie, B., Joshi, A.U., Minhas, P.S., Mukherjee, R., Andreasson, K.I., Mochly-Rosen, D., 2020. Mitochondrial dysfunction mediated through dynamin-related protein 1 (Drp1) propagates impairment in blood brain barrier in septic encephalopathy. J. Neuroinflammation 17 (1), 36. https://doi.org/10.1186/s12974-019-1689-8.

Horewicz, V.V., Crestani, S., de Sordi, R., Rezende, E., Assreuy, J., 2015. FPR2/ALX activation reverses LPS-induced vascular hyporeactivity in aorta and increases survival in a pneumosepsis model. Eur. J. Pharmacol. 5 https://doi.org/10.1016/j.ejphar.2014.11.026, 746- 267-73.

Hosokawa, K., Gaspard, N., Su, F., Oddo, M., Vincent, J.L., Taccone, F.S., 2014. Clinical neurophysiological assessment of sepsis-associated brain dysfunction: a systematic review. Crit. Care 18 (6), 674. https://doi.org/10.1186/s13054-014-0674-y.

Hotchkiss, R.S., Moldawer, L.L., Opal, S.M., Reinhart, K., Turnbull, I.R., Vincent, J.L., 2016. Sepsis and septic shock. Nat. Rev. Dis. Prim. 30 (2), 16045 https://doi.org/10.1038/nrdp.2016.45.

Isingrini, E., Camus, V., Le Guisquet, A.M., Pingaud, M., Devers, S., Belzung, C., 2010. Association between repeated unpredictable chronic mild stress (UCMS) procedures with a high fat diet: a model of fluoxetine resistance in mice. PLoS One 28 (4), e10404. https://doi.org/10.1371/journal.pone.0010404, 5.

Iwashyna, T.J., Ely, E.W., Smith, D.M., Langa, K.M., 2010. Long-term cognitive impairment and functional disability among survivors of severe sepsis. JAMA 304 (16), 1787–1794. https://doi.org/10.1001/jama.2010.1553.

Kaukonen, K.M., Bailey, M., Suzuki, S., Pilcher, D., Bellomo, R., 2014. Mortality related to severe sepsis and septic shock among critically ill patients in Australia and New Zealand, 2000-2012. JAMA 311 (13), 1308–1316. https://doi.org/10.1001/jama.2014.2637.

Kilkenny, C., Browne, W., Cuthill, I.C., Emerson, M., Altman, D.G., 2010. NC3Rs Reporting Guidelines Working Group. Animal research: reporting in vivo experiments: the ARRIVE guidelines. Br. J. Pharmacol. 160 (7), 1577–1579. https://doi.org/10.1111/j.1476-5381.2010.00872.x.

Machado, G.B., de Assis, M.C., Leão, R., Saliba, A.M., Silva, M.C., Suassuna, J.H., de Oliveira, A.V., Plotkowski, M.C., 2010. ExoU-induced vascular hyperpermeability and platelet activation in the course of experimental Pseudomonas aeruginosa pneumosepsis. Shock 33 (3), 315–321. https://doi.org/10.1097/SHK.0b013e3181b2b0f4.

Mervyn, S.M.D., Deutschman, C.S., Seymour, C.W., Shankar-Hari, M., Annane, D., Bauer, M., Bellomo, R., Bernard, G.R., Chiche, J.D., Coopersmith, C.M., Hotchkiss, R. S., Levy, M.M., Marshall, J.C., Martin, G.S., Opal, S.M., Rubenfeld, G.D., van der Poll, T., Vincent, J.L., Angus, D.C., 2016. The third international consensus definitions for sepsis and septic shock (Sepsis-3). JAMA 315 (8), 801–810. https://doi.org/10.1001/jama.2016.0287.

Michels, M., Abatti, M.R., Ávila, P., Vieira, A., Borges, H., Carvalho Junior, C., Wendhausen, D., Gasparotto, J., Tiefensee Ribeiro, C., Moreira, J.C.F., Gelain, D.P., Dal-Pizzol, F., 2020. Characterization and modulation of microglial phenotypes in an animal model of severe sepsis. J. Cell Mol. Med. 24 (1), 88–97. https://doi.org/10.1111/jcmm.14606.

Moraes, C.A., Santos, G., de Sampaio e Spohr, T.C., D'Avila, J.C., Lima, F.R., Benjamim, C.F., Bozza, F.A., Gomes, F.C., 2015. Activated microglia-induced deficits in excitatory synapses through IL-1β: implications for cognitive impairment in sepsis. Mol. Neurobiol. 52 (1), 653–663. https://doi.org/10.1007/s12035-014-8868-5.

Mu-Huo, J., Lei, L., Gao, D.P., Tong, J.H., Wang, Y., Yang, J.J., 2020. Neural network disturbance in the medial prefrontal cortex might contribute to cognitive impairments induced by neuroinflammation. Brain Behav. Immun. 89, 133–144. https://doi.org/10.1016/j.bbi.2020.06.001.

Pazini, F.L., Cunha, M.P., Azevedo, D., Rosa, J.M., Colla, A., de Oliveira, J., Ramos-Hryb, A.B., Brocardo, P.S., Gil-Mohapel, J., Rodrigues, A.L.S., 2017. Creatine prevents corticosterone-induced reduction in hippocampal proliferation and differentiation: possible implication for its antidepressant effect. Mol. Neurobiol. 54 (8), 6245–6260. https://doi.org/10.1007/s12035-016-0148-0.

Pellow, S., Chopin, P., File, S.E., Briley, M., 1985. Validation of open: closed arm entries in an elevated plus-maze as a measure of anxiety in the rat. J. Neurosci. Methods 14 (3), 149–167. https://doi.org/10.1016/0165-0270(85)90031-7.

Percie du Sert, N., Hurst, V., Ahluwalia, A., Alam, S., Avey, M.T., Baker, M., et al., 2020. The ARRIVE guidelines 2.0: updated guidelines for reporting animal research. PLoS Biol. 18 (7), e3000410 https://doi.org/10.1371/journal.pbio.3000410.

Pizzagalli, D.A., 2014. Depression, stress, and anhedonia: toward a synthesis and integrated model. Annu. Rev. Clin. Psychol. 10, 393–423. https://doi.org/10.1146/annurev-clinpsy-050212-185606.

Planchez, B., Surget, A., Belzung, C., 2019. Animal models of major depression: drawbacks and challenges. J. Neural Trans. J (Vienna) 26 (11), 1383–1408. https://doi.org/10.1007/s00702-019-02084-y.

Prager, G., Hadamitzky, M., Engler, A., Doenlen, R., Wirth, T., Pacheco-López, G., Krügel, U., Schedlowski, M., Engler, H., 2013. Amygdaloid signature of peripheral immune activation by bacterial lipopolysaccharide or staphylococcal enterotoxin B. J. Neuroimmune Pharmacol. 8 (1), 42–50. https://doi.org/10.1007/s11481-012-9373-0.

Prescott, H.C., Angus, D.C., 2018. Enhancing recovery from sepsis: a review. JAMA 319 (1), 62–75. https://doi.org/10.1001/jama.2017.17687.

Probst, J.J., Martins, G.H.C., Dos Santos Sumar, A.H., Vieira, A.M., Bion, M., Bobinski, F., Horewicz, V.V., Martins, D.F., Dos Santos, A.R.S., Bonorino, K.C., Luiz Dafre, A., de Camargo Hizume Kunzler, D., 2019. Pulmonary and muscle profile in pneumosepsis: a temporal analysis of inflammatory markers. Cytokine 114, 128–134. https://doi.org/10.1016/j.cyto.2018.11.012.

Prut, L., Belzung, C., 2003. The open field as a paradigm to measure the effects of drugs on anxiety-like behaviors: a review. Eur. J. Pharmacol. 463 (1–3), 3–33. https://doi.org/10.1016/s0014-2999(03)01272-x.

Radu, M., Chernoff, J., 2013. An in vivo assay to test blood vessel permeability. JoVE 73, e50062. https://doi.org/10.3791/50062.

Richwine, A.F., Parkin, A.O., Buchanan, J.B., Chen, J., Markham, J.A., Juraska, J.M., Johnson, R.W., 2008. Architectural changes to CA1 pyramidal neurons in adult and aged mice after peripheral immune stimulation. Psychoneuroendocrinology 33 (10), 1369–1377. https://doi.org/10.1016/j.psyneuen.2008.08.003.

Riel, D., Verdijk, R., Kuiken, T., 2015. The olfactory nerve: a shortcut for influenza and other viral diseases into the central nervous system. J. Pathol. 235 (2), 277–287. https://doi.org/10.1002/path.4461.

Rodgers, R.J., Dalvi, A., 1997. Anxiety, defence and the elevated plus-maze. Neurosci. Biobehav. Rev. 21 (6), 801–810. https://doi.org/10.1016/s0149-7634(96)00058-9.

Rudd, K.E., Johnson, S.C., Agesa, K.M., Shackelford, K.A., Tsoi, D., Kievlan, D.R., et al., 2020. Global, regional, and national sepsis incidence and mortality, 1990-2017: analysis for the Global Burden of Disease Study. Lancet 395 (10219), 200–211. https://doi.org/10.1016/S0140-6736(19)32989-7.

Russ, T.C., Kivimäki, M., Batty, G.D., 2020. Respiratory disease and lower pulmonary function as risk factors for dementia: a systematic review with meta-analysis. Chest 157 (6), 1538–1558. https://doi.org/10.1016/j.chest.2019.12.012.

Russell, J.A., Singer, J., Bernard, G.R., Wheeler, A., Fulkerson, W., Hudson, L., Schein, R., Summer, W., Wright, P., Walley, K.R., 2000. Changing pattern of organ dysfunction in early human sepsis is related to mortality. Crit. Care Med. 28 (10), 3405–3411. https://doi.org/10.1097/00003246-200010000-00005.

Sakr, Y., Jaschinski, U., Wittebole, X., Szakmany, T., Lipman, J., Ñamendys-Silva, S.A., Martin-Loeches, I., Leone, M., Lupu, M.N., Vincent, J.L., ICON Investigators, 2018. Sepsis in intensive care unit patients: worldwide data from the intensive care over nations audit. Open Forum Infect. Dis. 5 (12), ofy313. https://doi.org/10.1093/ofid/ofy313.

Salluh, J.I., Soares, M., Teles, J.M., Ceraso, D., Raimondi, N., Nava, V.S., Blasquez, P., Ugarte, S., Ibanez-Guzman, C., Centeno, J.V., Laca, M., Grecco, G., Jimenez, E., Árias-Rivera, S., Duenas, C., Rocha, M.G., 2010. Delirium epidemiology in critical care study group. Delirium epidemiology in critical care (DECCA): an international study. Crit. Care 14 (6), R210. https://doi.org/10.1186/cc9333.

Schuler, A., Wulf, D.A., Lu, Y., Iwashyna, T.J., Escobar, G.J., Shah, N.H., Liu, V.X., 2018. The impact of acute organ dysfunction on long-term survival in sepsis. Crit. Care Med. 46 (6), 843–849. https://doi.org/10.1097/CCM.0000000000003023.

Seymour, C.W., Liu, V.X., Iwashyna, T.J., Brunkhorst, F.M., Rea, T.D., Scherag, A., Rubenfeld, G., Kahn, J.M., Shankar-Hari, M., Singer, M., Deutschman, C.S., Escobar, G.J., Angus, D.C., 2016. Assessment of clinical criteria for sepsis: for the third international consensus definitions for sepsis and septic shock (Sepsis-3). JAMA 315 (8), 762–774. https://doi.org/10.1001/jama.2016.0288.

Sharshar, T., Bozza, F., Chrétien, F., 2014. Neuropathological processes in sepsis. Lancet Neurol. 13 (6), 534–536. https://doi.org/10.1016/S1474-4422(14)70064-X.

Simon, P., Dupuis, R., Costentin, J., 1994. Thigmotaxis as an index of anxiety in mice. Influence of dopaminergic transmissions. Behav. Brain Res. 61 (1), 59–64. https://doi.org/10.1016/0166-4328(94)90008-6.

Singer, B.H., Newstead, M.W., Zeng, X., Cooke, C.L., Thompson, R.C., Singer, K., Ghantasala, R., Parent, J.M., Murphy, G.G., Iwashyna, T.J., Standiford, T.J., 2016. Cecal ligation and puncture results in long-term central nervous system myeloid inflammation. PLoS One 11 (2), e0149136. https://doi.org/10.1371/journal.pone.0149136.

Singer, M., Deutschman, C.S., Seymour, C.W., Shankar-Hari, M., Annane, D., Bauer, M., et al., 2016. The third international consensus definitions for sepsis and septic shock (Sepsis-3). JAMA 315 (8), 801–810. https://doi.org/10.1001/jama.2016.0287.

Soares, A.C., Souza, D.G., Pinho, V., Vieira, A.T., Nicoli, J.R., Cunha, F.Q., Mantovani, A., Reis, L.F., Dias, A.A., Teixeira, M.M., 2006. Dual function of the long pentraxin PTX3 in resistance against pulmonary infection with Klebsiella pneumoniae in transgenic mice. Microb. Infect. 5, 1321–1329. https://doi.org/10.1016/j.micinf.2005.12.017.

Sonneville, R., Verdonk, F., Rauturier, C., Klein, I.F., Wolff, M., Annane, D., Chretien, F., Sharshar, T., 2013. Understanding brain dysfunction in sepsis. Ann. Intensive Care 3 (1), 15. https://doi.org/10.1186/2110-5820-3-15.

Sordi, R., Menezes-de-Lima, O., Della-Justina, A.M., Rezende, E., Assreuy, J., 2013. Pneumonia-induced sepsis in mice: temporal study of inflammatory and cardiovascular parameters. Int. J.Exp. Pathol. 94 (2), 144–155. https://doi.org/10.1111/iep.12016.

Steru, L., Chermat, R., Thierry, B., Simon, P., 1985. The tail suspension test: a new method for screening antidepressants in mice. Psychopharmacology (Berl) 85 (3), 367–370. https://doi.org/10.1007/BF00428203.

Sumar, A.H.S., Vieira, A.M., Martins, G.H.C., Probst, J.J., Martins, D.F., Bobinski, F., Horewicz, V.V., Mack, J.M., Danielli, N.M., Cunha, M.P., Assreuy, J., Bonorino, K.C., Goethel, M.F., Domenech, S.C., Dafre, A.L., Kunzler, D.C.H., 2021. Aerobic exercise ameliorates survival, clinical score, lung inflammation, DNA and protein damage in septic mice. Cytokine 140, 155401. https://doi.org/10.1016/j.cyto.2020.155401.

Tsuruta, R., Oda, Y., 2016. A clinical perspective of sepsis-associated delirium. J. Intens. Care 4, 18. https://doi.org/10.1186/s40560-016-0145-4.

Van der Poll, T., Van de Veerdonk, F.L., Scicluna, B.P., Netea, M.G., 2017. The immunopathology of sepsis and potential therapeutic targets. Nat. Rev. Immunol. (7), 407–420. https://doi.org/10.1038/nri.2017.36.

Venet, F., Monneret, G., 2017. Advances in the understanding and treatment of sepsis-induced immunosuppression. Nat. Rev. Nephrol. 14 (2), 121–137. https://doi.org/10.1038/nrneph.2017.165.

Wang, J., Song, R., Dove, A., Qi, X., Ma, J., Laukka, E.J., Bennett, D.A., Xu, W., 2022. Pulmonary function is associated with cognitive decline and structural brain differences. Alzheimers Dement 18 (7), 1335–1344. https://doi.org/10.1002/alz.12479.

Westhoff, D., Engelen-Lee, J.Y., Hoogland, I.C.M., Aronica, E.M.A., van Westerloo, D.J., van de Beek, D., van Gool, W.A., 2019. Systemic infection and microglia activation: a prospective postmortem study in sepsis patients. Immun. Ageing 2019 16, 18. https://doi.org/10.1186/s12979-019-0158-7.

Wilhelms, S.B., Huss, F.R., Granath, G., Sjöberg, F., 2010. Assessment of incidence of severe sepsis in Sweden using different ways of abstracting International Classification of Diseases codes: difficulties with methods and interpretation of results. Crit. Care Med. 38 (6), 1442–1449. https://doi.org/10.1097/CCM.0b013e3181de4406.

Willis, E.F., MacDonald, K.P.A., Nguyen, Q.H., Garrido, A.L., Gillespie, E.R., Harley, S.B. R., Bartlett, P.F., Schroder, W.A., Yates, A.G., Anthony, D.C., Rose-John, S., Ruitenberg, M.J., Vukovic, J., 2020. Repopulating microglia promote brain repair in an IL-6-dependent manner. Cell 180 (5), 833–846.e16. https://doi.org/10.1016/j.cell.2020.02.013. PMID: 32142677.

Wu, J., Cai, Y., Wu, X., Ying, Y., Tai, Y., He, M., 2021. Transcardiac perfusion of the mouse for brain tissue dissection and fixation. Bio Protocol. 11 (5), e3988 https://doi.org/10.21769/BioProtoc.3988.

Xin, Y., Tian, M., Deng, S., Li, J., Yang, M., Gao, J., Pei, X., Wang, Y., Tan, J., Zhao, F., Gao, Y., Gong, Y., 2023. The key drivers of brain injury by systemic inflammatory responses after sepsis: microglia and neuroinflammation. Mol. Neurobiol. 60 (3), 1369–1390. https://doi.org/10.1007/s12035-022-03148-z.